Universal graph representation of stabilizer codes

Andrey Boris Khesin,[1, *] Jonathan Z. Lu,[1, †] and Peter W. Shor[1, ‡]

[1]*Department of Mathematics, Massachusetts Institute of Technology, Cambridge, MA*

(Dated: December 20, 2024)

Abstract

While stabilizer tableaus have proven exceptionally useful as a descriptive tool for additive quantum codes, they otherwise offer little guidance for concrete constructions or coding algorithm analysis. We introduce a representation of $[\![n, k]\!]$ stabilizer codes as graphs with certain structures. Specifically, the graphs take a semi-bipartite form wherein k "input" nodes map to n "output" nodes, such that output nodes may connect to each other but input nodes may not. Intuitively, the graph's input-output edges represent information propagation of the encoding circuit, while output-output edges represent the code's entanglement structure. We prove that this graph representation is in bijection with tableaus and give an efficient compilation algorithm that transforms tableaus into graphs. We then show that this map is efficiently invertible, which gives a new universal recipe for code construction by way of finding graphs with sufficiently nice properties.

The graph representation gives insight into both code construction and algorithms. To the former, we argue that graphs provide a flexible platform for building codes particularly at smaller (non-asymptotic) scales. We construct as examples constant-size codes, e.g. a $[\![54, 6, 5]\!]$ code and a family of $[\![n, \Theta(\frac{n}{\log n}), \Theta(\log n)]\!]$ codes. We also leverage graphs in a probabilistic analysis to extend the quantum Gilbert-Varshamov bound into a three-way distance-rate-weight tradeoff. To the latter, we show that key coding algorithms—distance approximation, weight reduction, and decoding—are unified as instances of a single optimization game on a graph. Moreover, key code properties such as distance, weight, and encoding circuit depth, are all controlled by the graph degree. We give efficient algorithms for producing simple encoding circuits whose depths scale as twice the degree and for implementing logical diagonal and certain Clifford gates with non-constant but reduced depth. Finally, we construct a simple efficient decoding algorithm and prove a performance guarantee for a certain class of graphs, including the $[\![n, \Theta(\frac{n}{\log n}), \Theta(\log n)]\!]$ code. These results give evidence that graphs are generically useful for the study of stabilizer codes and their practical implementations.

---

[*] khesin@mit.edu

[†] lujz@mit.edu

[‡] shor@math.mit.edu

I. INTRODUCTION

Most quantum algorithms which are believed to provide significant speedups to certain computational problems require both many qubits and error correction to succeed in practice [1–8]. As advancements in the experimental scaling of quantum computers have steadily marched forward, the problem of designing good quantum codes for the practical implementation of various quantum algorithm has in turn become of more pressing interest [9–13].

With a few exceptions, stabilizer codes have emerged as one of the most intensely studied families of codes due to their simple description [8, 14–19]. Roughly speaking, stabilizer codes are the quantum analogue of linear codes for classical computing. More precisely, a $[\![n, k]\!]$ stabilizer code encodes k logical qubits to n physical qubits by embedding 2^k logical degrees of freedom into a subspace defined as the simultaneous $+1$ eigenspace of $n-k$ n-qubit Pauli operators, known as the stabilizers. Stabilizers comprise a considerably large class of quantum codes, including all CSS codes [20, 21].

Generally, a stabilizer code is specified by the *stabilizer tableau*, the $n-k$ Pauli operator strings which define the code space. This description is simple and elegant, and has led to remarkable results such as the Gottesman-Knill theorem [22], which efficiently simulates any Clifford operation classically, and the quantum Gilbert-Varshamov bound [8], which proves by a probabilistic technique that asymptotically good stabilizer codes exist. At the same time, the stabilizer tableau representation is prohibitive in many other ways. Without further structure, it is unclear as to how one might construct desirable codes by simply writing down a clever collection of $n-k$ Pauli strings, or how one might devise and analyze coding algorithms for a given tableau. For this reason, much of the constructive effort in quantum coding theory has relied on developing sophisticated CSS-type product operations that generate CSS codes from nice classical codes, and relying on classical algorithm analysis for inspiration [21, 23–25].

In this paper, we argue that a different approach based on graphs to represent stabilizer codes may also prove useful for the development and analysis of quantum codes. The employment of graphs in code construction has a rich history in coding theory. Classically, Tanner graphs, which encode a classical linear code into a bipartite graph, built the bridge between expander graphs and classical codes and significantly contributed to modern classical cod-

3

ing [26]. In the quantum realm, graph reasoning—specifically the topological structure of Euclidean lattices with periodic boundary conditions—motivated the development of the toric and other surface codes [27, 28]. The toric code was even shown to be efficiently decoded by way of classical graph algorithms, in particular Edmonds' minimum weight perfect matching [29, 30]. Outside of quantum coding, tensor networks have played a key role in quantum simulation and algorithm design.

The critical contributions of graphs in both classical and quantum coding in many specific constructive cases naturally lead to the questions of (a) what the most general graph techniques on stabilizer codes are and (b) how useful such a representation is for a variety of important coding tasks.

A.   Contributions, scope, and conjectures

This work takes a first step in answering both such questions. Our first contribution, in the direction of the first question, is the development of a simple graph representation of all stabilizer codes. The general structure of the graph is known as an *encoder-respecting form*, which has the structure of a semi-bipartite graph that maps k input-representing nodes to n output-representing nodes. By semi-bipartite, we mean that inputs may not be connected but outputs generically may. Informally, our result may be stated as the following.

Theorem I.1 (Informal). Every stabilizer code is essentially uniquely represented by an encoder-respecting graph satisfying some rules, and conversely every such graph essentially uniquely represents a stabilizer code. There is an efficient compilation algorithm that maps tableaus to graphs in $O(n^3)$ time and vice versa in $O(n^2)$ time.

The precise version of Theorem I.1 is given in Sections II and IV. This result establishes that our graph representation is sufficiently general to universally represent all stabilizer codes. We devised the compilation algorithm from tableaus to graphs in part for the study of graph properties of well-known codes. As examples, we compile the famous 5-qubit, 7-qubit, and 9-qubit quantum codes and show that each take simple geometric forms respectively of a cone, cube, and tree-star. Conversely, Theorem I.1 enables us to essentially transform any semi-bipartite graph into a stabilizer code, in such a way that (a) any stabilizer code can be constructed this way and (b) the properties of the code are tied to the properties of the

4

graph. As a consequence, we can leverage the tools of graph theory and graph algorithms to study stabilizer codes. We show that the key properties of a stabilizer code are controlled in a unified way, namely by the corresponding graph's degree.

Theorem I.2 (Informal)**.** Let G be a graph and $C(G)$ the corresponding code. The following hold.

(1) The distance of $C(G)$ is bounded above by the min-degree of G.

(2) The stabilizer tableau produced by the algorithm in Theorem I.1 has weights bounded by a quadratic function of the degree of certain nodes in G.

(3) There exists an efficient algorithm which produces an encoding circuit for $C(G)$ whose depth is bounded by (up to a small additive constant) twice the maximum degree of G.

(4) Every constant-depth diagonal gate and the $\sqrt{X}$ can be implemented logically in $C(G)$ with a circuit of depth, respectively, about (up to an additive constant) twice the max-degree and the max-degree.

The formal versions of these statements are given in Section IV.

To further strengthen the connection between graphs and codes, we next define a simple, one-player optimization-type game on a graph which we call quantum lights out (QLO), in Section IV. We prove that QLO unifies many important tasks in quantum coding, which opens a path towards the study of coding algorithms via their correspondence to approximately optimal QLO strategies.

Theorem I.3 (Informal)**.** Many coding algorithms such as distance approximation, stabilizer weight reduction, and decoding are all approximately optimal strategies for QLO games.

The above results demonstrate that graphs in many senses unify various aspects of stabilizer coding in a simple manner. Overall, we give four pieces of evidence that graphs serve as a useful representation. In the first, which we discussed above, we show that graphs enable efficient algorithms which produce encoding and logical-operator circuits whose depth are controlled by the degree. Later on, when we study decoding, we are able to bound the depths directly by the distance of the code for graphs which satisfy a certain property.

In the second aspect, we explore the geometric and topological properties of graph as tools for building codes. Noticing that simple geometric solids realize celebrated quantum codes, we construct codes based on other such solids, including platonic solids and topological transformations of them. For simpler constructions, we are able to calculate the distance by direct computation. As an example, we produce a non-CSS stabilizer code from a dodecahedron, which has parameters $[\![16, 4, 3]\!]$. We also construct a $[\![54, 6, 5]\!]$ code by lifting the icosahedron to a covering space. For more complicated constructions, we use more indirect analytical techniques based on decoding. The main advantage of graphs as a constructive tool is their flexibility: we show that graphs enable us to more easily produce codes that have a desired numerical distance, by finding graphs which have a similar degree. Graphs also can be chosen to immediately satisfy desired experimental constraints based on locality, geometric structure, etc. Thus, the graph representation may prove helpful tools for code construction at constant-size scales fit for experimental use.

Our third avenue is decoding. In general, we believe that the graph representation serves as an excellent guide for the design of decoding algorithms. Historical evidence of minimum-weight perfect matching on the surface code suggests that graphs are indeed helpful. In this paper, we take a first step in that direction by designing a decoder that employs a simple greedy strategy on the QLO game. We give a general condition on graphs, which we call its *sensitivity*, that sufficiently characterizes a graph's amenity to be decoded well greedily. For concreteness, we also design a simple family of $[\![\frac{m2^m}{m+1}, \frac{2^m}{m+1}]\!]$ codes, which we call the hypercube codes. Their distance is provably at most m, but we show that the decoder can correct at least $m/4$ errors on it, so that the distance is also at least $m/2$ (up to a ± 1 additive constant). We conjecture, however, that a more careful analysis can prove that the distance is actually m. Assuming this conjecture, a small case of the hypercube code family is $[\![112, 16, 7]\!]$. Moreover, our results imply a lower bound on the distance in terms of the degree, which in turn lead to bounds on encoding circuit depth, logical operator circuit depth, and stabilizer weight entirely in terms of distance.

Finally, we exploit the structure of graphs to give a more fine-grained argument about random codes. By randomly connecting edges of our graphs, we give a large class of codes for which almost all members satisfy a tradeoff between rate, distance, and stabilizer weight. This extends the result of the quantum Gilbert-Varshamov bound, which shows by a coarse-

grained probabilistic stabilizer tableau analysis a similar result with a rate-distance tradeoff but always large stabilizer weight. Such a result further exemplifies that graphs enable greater flexibility in code analysis.

Our paper argues at a very general scope, namely at the level of all stabilizer codes. The universality of our work therefore has limitations that do not exist for highly specific quantum low-density parity check (qLDPC) constructions. In particular, even when optimized as much as possible with known techniques, code properties such as check weight, encoding circuit depth, and logical operator circuit depth, will scale with the degree and therefore the code parameters, though not necessarily by a great deal (logarithmic, for example). Thus, our intention is not to use the graph representation as a means for continued study into asymptotically good qLDPC codes with very large constants in the manner of Refs. [31–34]. Rather, we consider our work to be complementary to qLDPC in the sense that we give general insight into stabilizer codes and new flexible ways to construct codes that may be tailored specifically for a given experimental implementation. As an example, a future quantum long-term memory device may seek a particular large numerical distance threshold but care little for comparably large check weights if the measurement error is sufficiently small. This philosophy underpins our explicit construction of codes which have desirable properties at small scales. We believe also that further applications of graph theoretical techniques may further improve the techniques in this paper to build increasingly practical recipes for code constructions that flexibly adapt to experimental constraints.

More generally, we argue that graph theory provides a promising path forward *generally* across avenues of quantum coding theory. Recent breakthroughs in qLDPC codes, for example, have relied on graphs in their construction to generalize the use of surface code lattices [28]. Perhaps further generalizations of these specific types of constructive techniques, as well as less universal but more fine-grained (i.e. finding certain graph constructions which map to codes in such a way that some properties scale favorably or not at all with parameters) refinements of the universal graph representation will lead to new constructions of and insights into quantum codes.

B. Related Work

Graph forms have been exploited in many ways in the quantum computation literature, most generally via tensor network representations. One simple case of a graph representation is a graph state. Hu and Khesin [35] has produced a generalized graph state representation of stabilizer *states*, i.e. a stabilizer code with 0 logical qubits. Our reduction from tableau to graph utilizes insights from Hu and Khesin [35], and in the special case of $n = k$ in our work, there is a transformation that reduces our tableau-to-graph map to their corresponding map. We remark that McElvanney and Backens [36], building upon Hu and Khesin [35], derived a different unique canonical form for stabilizer states that are particularly convenient for measurement-based quantum computation. Independently, Yu *et al.* [37] also utilized graph theory in quantum coding, albeit at a much more general level (including non-stabilizer codes) for constructive and classification purposes.

Parts of our work—particularly the reduction from tableau to graph—utilize rules and notation from the ZX calculus. Recent works have also explored the use of ZX calculus to diagrammatically express quantum codes. A recent work of Kissinger [38] developed independently of this work also constructs diagrammatic forms for *CSS codes*. Their forms are substantially different for ours and serve a different purpose. Primarily, Kissinger establishes a correspondence between CSS codes and ZX diagrams, by non-uniquely mapping CSS codes to such diagrams and mapping a subset of the ZX diagrams (the phase-free ones) to CSS codes. The tableau-to-graph portion of our work extends the conceptual idea of diagrammatic forms inspired by ZX calculus to all stabilizer codes, but takes a significantly different approach and utilizes the result for constructive and algorithmic purposes.

More generally, ZX calculus approaches to quantum error correction have been considered in various ways. Two relatively recent works which utilize the ZX calculus exemplify these different approaches. In the first way, Wu *et al.* [39] represent specifically graph codes with ZX calculus diagrams. This approach, while not general to stabilizer or CSS codes, has shown promise in code analysis. The second, due to Chancellor *et al.* [40], uses the ZX calculus specifically to quantize classical codes in the spirit of CSS code construction. Both of these works give evidence that graphs enable new insights into quantum coding, both in their construction and analysis, and thus motivate our completely general theory

8

of graph representations. Moreover, aside from our tableau-to-graph reduction algorithm which does use elements of the ZX calculus, our work builds everything essentially only from the standard definition graphs. We emphasize that the graphical diagrams of the ZX calculus require additional structure. Therefore, graph representations further simplify related previous works that also devise similar representations based on the ZX calculus. The specific motivations, applications, and analysis in these papers are also distinct from those in this work.

Building upon a preliminary earlier version of this work, Khesin and Li [41] conducted further analysis of graph representations in the special case of CSS codes, wherein the graphs become bipartite. They specifically analyzed different ways to further simplify the graph representation and potential advantages in doing so.

II. FROM TABLEAUS TO GRAPHS

We begin by constructing the general graph form and compiling any stabilizer tableau into such a graph. More precisely, we will compile an equivalence class of encoding Clifford circuits corresponding to an equivalence class of stabilizer tableaus, and at the end of this section we discuss how to compile starting with a tableau [18]. As a starting point, we appeal to the ZX-calculus, a graph language for vectors that has become of great interest in quantum information research [38, 42–46]. The ZX-calculus produces visual diagrams that represent quantum states, circuits, and more. As with any formal logical system, the ZX calculus has a set of rules which may be iteratively applied to transform diagrams into equivalent diagrams. These rules are representations of identities in quantum circuits. The ZX-calculus has become of more interest than ever in fault-tolerant quantum computation and quantum compiler theory because it can explicitly visualize quantum properties such as entanglement in an intuitive manner. It has recently been applied to a host of quantum computation problems, including lattice surgery [47] and quantum optimization [48]. Importantly, the ZX-calculus is, for stabilizer tableaus, complete (equalities of tableaus can be derived from corresponding ZX diagrams), sound (vice versa), and universal (every quantum operation can be expressed in the ZX-calculus) [42, 49].

We are consequently motivated to leverage the ZX calculus as an intermediate step in

the development of a graph presentation. Ultimately, our graphs will be simple graphs and not the more complicated and structured diagrams in the ZX calculus. The diagrams that we map our circuits into are a subset of ZX diagrams that are equivalent by a simple transformation to graphs. To more clearly elucidate the transformation from tableau to graph, we construct the map from a composition of simpler maps. In particular, we first convert the tableau into a circuit. Next we show that up to an equivalence relation, we can efficiently biject the circuits into a class of ZX diagrams of a certain form that satisfies four rules. We thus denote these diagrams *ZX canonical forms* (ZXCFs). Lastly, we remove unnecessary structure from ZXCFs to obtain a graph representation of the code. This is pictorially represented by the following maps.

$$\text{Tableau} \longleftrightarrow \text{Encoder} \longleftrightarrow \text{ZXCF} \overset{\text{LE}}{\longleftrightarrow} \text{Graph}. \tag{1}$$

In absence of the last step, everything is completely invertible and has an interpretation as a unique compiler. For the last step, the map between ZXCFs and graphs is invertible modulo *local equivalence*; that is, modulo local (1-qubit) Clifford operations on the outputs. An immediate consequence for this ZXCF compiler is a diagrammatic method of testing equality between stabilizer codes.

We begin the formalism by noting that properties of a code depend only on the codespace, and thus there is a unitary degree of freedom on the logical space. In particular, encoding circuits for a given stabilizer tableau will produce the same stabilizer code if and only if they differ by an image. We therefore make the following definition.

Definition II.1. Two circuits are equivalent as *Clifford encoders* if they have the same image over all possible input states. Equivalently, $\mathcal{C}_1$ and $\mathcal{C}_2$ are equivalent encoders if there exists a unitary U acting on the inputs of the circuit such that $\mathcal{C}_1 = \mathcal{C}_2 U$ or $\mathcal{C}_2 = \mathcal{C}_1 U$.

Any reference we make to encoding circuits will either implicitly or explicitly refer to them up to this equivalence, and indeed they all map to the same stabilizer code.

A. ZX Canonical Form Construction

In the intermediate steps using ZX calculus rules, we follow the standard notation of ZX-calculus graph diagrammatics, specified in Backens [49]; we refer the reader there for the

basics of the ZX calculus and transformation rules.

A ZX diagram is a graph with additional structure. In particular, nodes may be either red or green, nodes may be decorated with local Clifford operators, and edges may be Hadamarded. Additionally, nodes may have a "free edge", an edge connected only to one node and dangling on the other side. Green nodes are associated with Z operators, and red with X. Each node may be associated with a local Clifford operator (which may be expressed as a phase which is a multiple of $\pi/2$), and each edge may have a Hadamard gate on it. We colour an edge blue if it has a Hadamard gate on it [50] (some papers use instead a line with a box, e.g. [49]). The circuit takes k input qubits to n output qubits, for $k \leq n$.

The specific structure of our graphs will be those in the following form.

Definition II.2. An *encoder-respecting form* $\mathcal{D}$ has only green (Z) nodes, and is structured as a *semi-bipartite graph*. A semi-bipartite graph has a left and right cluster, such that left-cluster nodes may have edges only to right-cluster nodes, but right-cluster nodes have no such restrictions. In our case, the left and right cluster are denoted as the input and output clusters, respectively. The input cluster $\mathcal{I}$ has k nodes associated with the k input qubits of the corresponding encoder, and the output cluster $\widetilde{\mathcal{O}}$ has n nodes. Each input node has a free (not connected to any other nodes) edge—the input edge. Similarly, each output node has a free output edge. The output edges are numbered from 1 to n—in order from left to right on an incomplete stabilizer tableau or top to bottom on Clifford circuit output wires. For convenience, we refer to the node v connected to an output edge numbered i as the output node numbered i.

The design of the encoder-respecting form graphically illustrates how information propagates from input to output (which edges connect $\mathcal{I}$ to $\widetilde{\mathcal{O}}$) as well as the entanglement structure (which edges connect $\widetilde{\mathcal{O}}$ to $\widetilde{\mathcal{O}}$) of the underlying encoder. We emphasize that this idea is only for intuition, as there exists equivalence transformation rules on ZX diagrams that appear to change the connectivity in nontrivial ways but are nonetheless the same diagram. Note that the structure of $\mathcal{D}$ gives rise to a natural binary "partial adjacency matrix" $M_{\mathcal{D}}$ of size $k \times n$, which describes the edges between $\mathcal{I}$ and $\mathcal{O}$ akin to the standard graph adjacency matrix.

Although this structure appears intuitively appealing, it is insufficient because there exists several equivalence transformations in the ZX calculus that yield an equivalent (but not
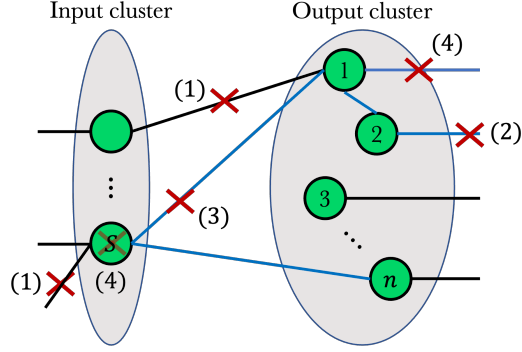
FIG. 1. Example of an encoder-respecting form and some ways it might violate the 4 rules.

obviously so) diagram. We therefore constrain an encoder-respecting form into a ZXCF via four additional rules. For notational convenience, we will interchangeably refer to applying an operation on a node's free edge as applying an operation on the node.

1. *Edge Rule*: The ZXCF must have exactly one Z-node per free edge and every internal edge must have a Hadamard on it.

2. *Hadamard Rule*: No output node v may both have a Hadamard gate on its output edge and have edges connecting v to lower-numbered nodes or input nodes.

3. *RREF Rule*: $M_{\mathcal{D}}$ must be in reduced row-echelon form (RREF).

4. *Clifford Rule*: Let $\mathcal{P} \subseteq \mathcal{O}$ be the nodes associated with the pivot columns of the RREF matrix $M_{\mathcal{D}}$, so that $|\mathcal{P}| = k$. The only local Cliffords allowed on nodes are $\{I, S, Z, SZ, H, HZ\}$, but there can be no operations at all on input or pivot nodes. There can be no input-input edges or pivot-pivot edges.

We have elected for emphasis to include the Z-nodes only constraint in the edge rule and the no input-input edges constraint in the Clifford rule even though these are redundant with that of the encoder-respecting form.

To provide some visual intuition on these 4 rules, Fig. 1 depicts a generic example of some possible violations to the rules. We define the four rules such that the ZXCF is homogeneous in node type and minimal in terms of decorated operators, number of edges. It can be shown [49, 51] that each of these rules corresponds to certain equivalence transformations. For example, row operations on $M_{\mathcal{D}}$ correspond to unitaries on the input. Rather than give

all the rules, we will directly devise an encoder to ZXCF map and prove that such a map is efficient and bijective.

Theorem II.3. Any Clifford encoder has a unique equivalent ZXCF satisfying the Edge, Hadamard, RREF, and Clifford rules. There exists an algorithm, running in worst-case $O(n^3)$ time, that on input a description of the Clifford encoder outputs a corresponding ZXCF. This map is bijective.

We briefly sketch the proof idea of Theorem II.3 but defer the details to Appendix A. The proof involves a series of transformations via ZX equivalence rules. In the first step, we apply an isomorphism between circuits and states, and proceed to apply a result of Hu and Khesin [35] to preliminarily represent the circuit as the ZX diagram of a corresponding state. We then transform the diagram into one representing a circuit, and carefully choose a series of equivalence transformations that iteratively force the diagram to satisfy a rule above without at the same time violating a different rule that has previously been satisfied. The resulting product is precisely a ZXCF. In fact, because the steps are equivalence transformations, distinct encoders map to distinct ZXCFs. The only remaining aspect of the proof of Theorem II.3 is whether this one-to-one map is bijective. We prove this claim in Section II B.

1. Tableau to encoder

There are numerous algorithms for mapping a stabilizer tableau into a Clifford encoding circuit [8]. If we quotient out operations which leave the code space invariant, then any such map is also bijective. We describe one such algorithm. For a $(n - k) \times n$ tableau, begin by drawing n output wires. At each step, we first simplify the tableau by applying a Clifford operation, and then measure out one of the qubits to remove one row and column from the tableau. Repeating inductively yields a Clifford circuit that takes k qubits to n qubits.

The procedure at each step begins by finding a Clifford operation U that turns the first stabilizer into $Z_1 = Z \otimes I \otimes \cdots \otimes I$, in the manner dictated by the Gottesman-Knill theorem. U is prepended to the circuit under construction. We then multiply the remaining rows by the first until the entire first column of the tableau has only I, with the exception of the first row. This can always be done, since the n-qubit Pauli operators in each row of the matrix

13

must commute. We then post-select on the $+1$ result of a computational basis measurement by applying $\langle 0|$ in the reverse direction. When reading the circuit in the forward direction, this is equivalent to initializing an ancillary qubit in the $|0\rangle$ state. The effect of U and the measurement is equivalent to applying $\frac{I+P}{2}$, where P is the first row of the stabilizer tableau. This is equivalent to post-selecting on the $+1$ measurement result of that stabilizer. Having measured the qubit, we remove its corresponding row and column from the tableau, and repeat on a tableau of $n-1$ qubits and $n-k-1$ rows, until there are no rows left, at which point the remaining k wires that have not been measured out become the input qubits in the circuit. We conclude by drawing k input wires for those qubits.

B. Proof of Canonicity

We next prove that our proposed ZXCF is indeed canonical. In other words, two equivalent stabilizer tableaus—generators of the same subspace of the n-qubit Hilbert space—will map to the same ZXCF. We proceed by counting the number of stabilizer tableaus and ZXCFs. For notational convenience, solely in this section, we will let k be the number of rows of the tableau rather than the number of inputs; that is, let $k \leftrightarrow n-k$.

First, the number of stabilizer tableaus with k stabilizers on n qubits is

$$\frac{\prod_{i=1}^{k} 2 \cdot 4^n / 2^{i-1} - 2 \cdot 2^{i-1}}{\prod_{i=1}^{k} 2^k - 2^{i-1}} = \prod_{i=1}^{k} \frac{2^{2n-i+2} - 2^i}{2^k - 2^{i-1}}. \tag{2}$$

For each row i, there are $2 \cdot 4^n$ possible Pauli strings (including the sign), but the requirement that they commute with previous rows divides the count by 2^{i-1}. Of these $2 \cdot 4^n / 2^{i-1}$ valid strings, 2^{i-1} strings are linear combinations of previous strings, with a factor of 2 for strings that differ by a sign from previous strings.

We have overcounted, however, since there are many ways to find a set of stabilizer generators for a particular tableau. In particular, when choosing a set of generators for a Clifford encoder, we have $2^k - 1$ choices for the first generator (subtracting the identity). There are then $2^k - 2$ ways of choosing the next element, as we cannot pick anything in the span of the elements chosen so far. Repeating inductively gives the denominator above.

Next, the number of ZXCF diagrams for the same n and k can be expressed by the

following fourfold recursive function f evaluated at $p = o = 0$.

$$f(n, k, p, o) = \begin{cases} 1 & \text{if } n = k = 0 \\ A_{n,k,p,o} + B_{n,k,p,o} & \text{else} \end{cases} \tag{3}$$

where

$$A_{n,k,p,o} = 2^o f(n-1, k, p+1, o) \tag{4}$$

if $n \neq k$ and $A_{n,k,p,o} = 0$ if $n = k$, and where

$$B_{n,k,p,o} = (2^{2p+o+2} + 2) f(n-1, k-1, p, o+1) \tag{5}$$

if $k \neq 0$ and $B_{n,k,p,o} = 0$ if $k = 0$.

This function is computed with a base case of an empty tableau when $n = k = 0$. Derivation of this function is left to Appendix B. We solve for an explicit form to obtain

$$f(n, k, p, o) = 2^{o(n-k)} \prod_{i=1}^{k} \frac{(2^{n+1} - 2^i)(2^{n-i+1+2p+o} + 1)}{2^k - 2^{i-1}}. \tag{6}$$

One can verify by standard induction that $f(n, k, 0, 0)$ gives the same expression as Eq. (2), proving that ZXCF is indeed canonical.

C. ZXCF to graph

In the final step, we reduce a ZXCF directly to a graph. We remark that any local Clifford operation must, by the Clifford rule, be placed only on non-pivot output nodes. However, local Cliffords do not change the weights of the set of correctable errors. Thus, local Cliffords do not change the code distance or any other code parameters. If we also quotient out this equivalence, we may remove all local Cliffords entirely. Since all internal edges have Hadamards, we can remove those as well and simply remember that they exist for inversion. Similarly, we can remove all free edges. The remaining diagram is identically a graph, specified entirely by a collection of nodes and edges. As a consequence, we have completed the map sequence from Eqn. (1), except for the graph to ZXCF map.

Theorem II.4. For any stabilizer code, there exists at least one equivalent code that has a presentation as a semi-bipartite graph with no local Clifford operations.

Moreover, we make the following observation.

Observation II.5. A code is CSS if and only if its graph is bipartite.

This can be seen by applying Hadamard gates to one of the two sets of vertices, which will split the stabilizers into X-only and Z-only sets.

III.   APPLICATION TO QUANTUM CODES

It is illuminating to observe the graph representation of well-known quantum codes. Not only does it inform of geometric structure embedded in the code, but it also provides a guide as to how such codes may be generalized. We provide three examples for study. Consider first the nine-qubit code, due to Shor [17], which uses 9 physical qubits to encode 1 logical qubit. The Shor code may be represented by the stabilizer tableau

$$
\begin{bmatrix}
Z & Z & I & I & I & I & I & I & I \\
Z & I & Z & I & I & I & I & I & I \\
I & I & I & Z & Z & I & I & I & I \\
I & I & I & Z & I & Z & I & I & I \\
I & I & I & I & I & I & Z & Z & I \\
I & I & I & I & I & I & Z & I & Z \\
X & X & X & X & X & X & I & I & I \\
X & X & X & I & I & I & X & X & X
\end{bmatrix}.
\tag{7}
$$

In Fig. 2, we give the graph representation in (a) and the ZXCF in (b). We denote in the ZXCF the input node with **I**, and the free edges are dotted for emphasis. In the graph presentation, the input node is blue and the outputs are black. We first examine the ZXCF. There are three identical sectors of the outputs, two with Hadamarded outputs and one without. This resembles our expectations from examination of the un-normalized qubit representation of the Shor code, $(|000\rangle \pm |111\rangle)^{\otimes 3}$. The graph, on the other hand, is a star-shaped tree. It is easy to imagine how one might extend the Shor code into an infinite family of graphs, namely by recursively giving every outer (leaf) node two children.

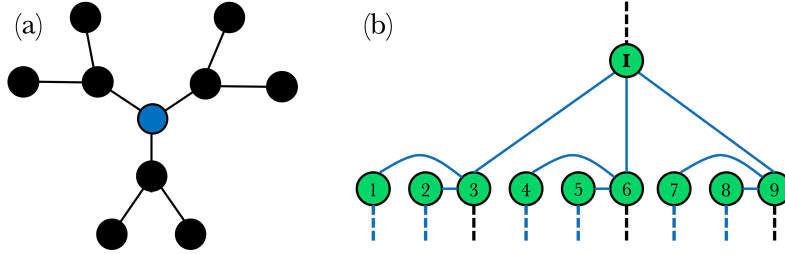Next, we compile Steane's seven-qubit code, a central construction in many fault-tolerant

16

FIG. 2. (a) Graph presentation and (b) ZXCF of the 9-qubit code. The input in the graph is shown in blue. Note that the graph encoder uses a slightly different basis as since its output edges do not contain Hadamard gates.

quantum computation schemes [20]. The code is represented by the following tableau:

$$
\begin{bmatrix}
I & I & I & X & X & X & X \\
I & X & X & I & I & X & X \\
X & I & X & I & X & I & X \\
I & I & I & Z & Z & Z & Z \\
I & Z & Z & I & I & Z & Z \\
Z & I & Z & I & Z & I & Z
\end{bmatrix}.
\tag{8}
$$

In our ZXCF, this code takes the form given in Fig. 3. In particular, the nodes of the diagram are simply the corners of a cube. A similar picture has been given in a different context in Duncan and Lucas [52]. The Steane code's generalization is also evident, via extensions into hypercubes of arbitrary dimension. We explore precisely such a coding scheme in Section V B.

We observe that the stabilizers of the 7-qubit code are positioned at exactly the 1-indices in the binary representation of a node label. We can see elegant symmetries in Fig. 3 with the positions of the nodes and their expressions in binary. The reason why the nodes adjacent to 0 are not 1, 2, and 4, (respectively 001, 010, and 100 in binary) is because the rules of the ZXCF require that the Hadamarded output edges not be connected to lower-numbered nodes.

As a final example we consider the five-qubit code, which is the smallest code one can achieve for correction of an arbitrary single-qubit error and has been studied experimen-
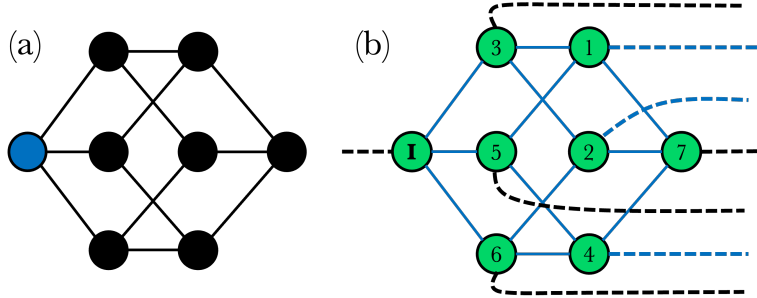
17

FIG. 3. (a) Graph presentation and (b) ZXCF of the 7-qubit code. The input in the graph is shown in blue. Note that the graph encoder uses a slightly different basis as since its output edges do not contain Hadamard gates.

tally [18, 53]. Its tableau representation is given by

$$
\begin{bmatrix}
X & Z & Z & X & I \\
I & X & Z & Z & X \\
X & I & X & Z & Z \\
Z & X & I & X & Z
\end{bmatrix}.
\tag{9}
$$

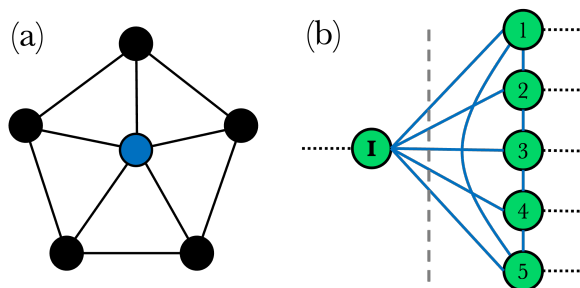Our procedure produces the ZXCF shown in Fig. 4.

FIG. 4. (a) Graph presentation and (b) ZXCF of the 5-qubit code. The input in the graph is shown in blue.

The 5-qubit code takes the shape of either a pentagon with an input in the middle or a cone, depending on how one sets up the graph. Consequently, a simple generalization is to use a n-gon, or equivalently add more nodes to the circle in the cone.

Such elegant and simple structure in the 5, 7, and 9-qubit codes suggest that other graphs with similar elegant structure may yield interesting quantum codes, either of constant size or in family. We explore this idea in Section V A.

IV. THE INVERSE MAP: FROM GRAPHS TO STABILIZER CODES

The bijective relation between stabilizer codes and graphs—particularly those in the ZX canonical form—give justification that graphs are at least as powerful as stabilizer tableaus for the expression of codes. In this section, we lay the foundation for the use of graphs as *constructive tools* for code design. Such a mapping from graphs to stabilizer tableaus can be viewed as an "inverse map" to the algorithm given in Section II B, with some caveats relating to the fact that not all graphs can be equivalently represented by ZXCFs and therefore not all graphs can be mapped into codes.

Let G be a graph with $n+k$ nodes, separated into k input nodes $\mathcal{I}$, a choice of k pivot nodes $\mathcal{P}$, and $n-k$ output nodes $\mathcal{O}$. To ensure that our operations are well-defined, there must exist equivalence operations that map G into a ZXCF. The only nontrivial restriction this requirement poses is on the choice of pivots. The RREF rule ensures that every distinct pivot is connected to exactly one distinct input; in other words, $\mathcal{P}$ and $\mathcal{I}$ are perfectly matched. Because row operations on the partial adjacency matrix are equivalences, it suffices to choose pivots such that there exists a row-reduced partial adjacency matrix $M_{\mathcal{D}}$ for which the chosen k pivot nodes correspond to the k pivot columns of $M_{\mathcal{D}}$. A simple example of this subtlety is shown in Fig. 5. Here, it is impossible to choose the first two outputs to be the pivots because the third output is forced to be a pivot when we row-reduce. Note, however, that this subtle restriction poses no issue if every distinct pivot we choose is already connected to exactly one distinct input (as in the case in Section V C) or if we can observe directly that the pivots we have chosen do correspond to the pivot columns after row reduction. Henceforth, we will denote G as a graph for which a set of valid pivots $\mathcal{P}$ have been specified alongside a set of input nodes $\mathcal{I}$.

Assuming the choice of $\mathcal{P}$ is valid, G will be equivalent to a ZXCF by a series of equivalence transformations. First, we place a free edge on every node and place a Hadamard on all internal edges, satisfying the edge rule. The Hadamard rule is vacuously satisfied, as we will not place any Hadamard on output nodes. We can row-reduce the partial adjacency matrix to satisfy the RREF rule. Next, we strip input-input edges, which are unitaries on the inputs and thus represent equivalent encoders. Lastly, as discussed in Section II, there is an equivalence relation that strips pivot-pivot edges. This procedure results in a ZXCF

19

$$M_{\mathcal{D}} = \begin{pmatrix} 1 & 1 & 0 \\ 1 & 1 & 1 \end{pmatrix} \qquad M_{\mathcal{D}} = \begin{pmatrix} 1 & 1 & 0 \\ 0 & 0 & 1 \end{pmatrix}$$
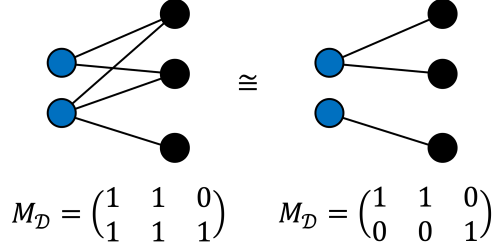
FIG. 5. A simple example for which the third output node is necessarily a pivot. The inputs are blue and outputs are black. The example is given on the left, and an equivalent graph is given on the right.

with no local Clifford on nodes at all. While there exist encoders that can only be expressed with local Clifford operations that this map cannot produce, the map can always produce a locally equivalent encoder, and is otherwise completely general.

In practice, we never transform our graphs into a ZXCF. The only transformation we shall make is endow every node with a free edge. This endowment enables a simpler description of operator actions on the graph. However, in our diagrams we will omit the free edges to reduce clutter. We can also strip input-input edges and pivot-pivot edges if desired for convenience. Aside from that, knowing that the graph is equivalent to a ZXCF, we can write down the stabilizer generators of its corresponding ZXCF directly. To do so, we first establish notation. Let $\Delta_{i=1}^{n} A_i = A_1 \Delta \cdots \Delta A_n$ for sets $A_1, \ldots, A_n$, where Δ is the symmetric difference. The symmetric difference is both commutative and associative, so this iterative procedure is well-defined. Consider some $v \in \mathcal{O}$. We define $i(v) = \{w \in \mathcal{I} \,|\, w \sim v\}$ the inputs connected to v and $p(v) = \{w \in \mathcal{P} \,|\, w \sim v\}$ the pivots connected to v, which each consist of only one vertex if v is a pivot or an input, respectively. For later use we similarly define $o(v) = \{w \in \mathcal{O} \,|\, w \sim v\}$, the set of non-pivot outputs connected to v. We also define $N_o(v) = \{w \in \mathcal{O} \cup \mathcal{P} \,|\, w \sim v\} = o(v) \cup p(v)$ the non-input neighbours of $v \in \mathcal{O}$, and more generally $N_o(A) = \Delta_{v \in A} N_o(v)$ and similarly for $i(A)$, $p(A)$, and $o(A)$. The symmetric difference is useful for correctly counting the parities of Pauli operations applied to certain nodes, i.e. if a Pauli is applied twice in the set, it is effectively not applied at all.

Let $X(w)$ be a Pauli on (the free edge of) node w, and $X(A) = \bigotimes_{v \in A} X(v)$; Z operators are defined analogously. Note that we may only directly apply operators to (the free edge of) output nodes because these are physical operators. With this notation, we define the

following map $\mathcal{S} : G \mapsto S$ from graph to stabilizer tableau, the output of which we call the *canonical stabilizers* of the code represented by G.

$$\mathcal{S} := \{X(v)Z(N_o(v))X(p(i(v)))Z(N_o(p(i(v))))\}_{v\in\mathcal{O}}. \tag{10}$$

Denote each stabilizer S_v for $v \in \mathcal{O}$. These stabilizers are readily seen to be a valid generating set. There are exactly $n-k$ generators, and all are independent because only S_v has a X on v. Every pair of stabilizers S_v and S_w also have even X-Z overlap–and thus commute—because the graphs are undirected. In principle, one could disregard the entirety of the previous section, *define* Eqn. (10) as a map from graphs to stabilizers, and explore their properties. However, it is unclear a priori from this approach how expressive such a class of stabilizers would be and the motivation behind such an assertion would be obscure. We next show that such a map generates precisely the stabilizer group of the encoder that the corresponding ZXCF of G represents. Because graphs do not have local Clifford operations associated to them, we can treat $\mathcal{S}$ as the inverse map from graph to ZXCF, modulo local Cliffords, i.e. up to local equivalence. To do so, we appeal to the two most fundamental equivalence rules of the ZX calculus. Indeed, we will use these rules many times in the course of our calculations.

Lemma IV.1 (ZX-calculus fundamental equivalences)**.** Let v be a Z-node in a ZX diagram. Operators may be placed on edges and associated with a on either side of the edge.

(1) If an operator placed on an internal edge between v and w is *associated* with v, it can be equivalently associated with w instead. However, if the internal edge is Hadamarded, the operator is flipped $X \leftrightarrow Z$ during this change of association. An operator placed on a free edge of v is vacuously associated with v.

(2) If a X operator is placed on an edge associated with v, it can be equivalently commuted through v into X's on *every other edge* (including the free edge) connected to v, each remaining associated with v.

(3) If a Z operator is placed on an edge associated to v, it may be equivalently commuted through as a Z on *any one* other edge associated to v, remaining associated to v.

The rules provided in Lemma IV.1 give a prescription for generating stabilizers. Fix $v \in \mathcal{O}$. First, place a X on the free edge of v. By rule (2), this X equivalently transforms

into X on all other edges connected to v, associating with v. For edges connecting v to a non-input node w, we re-associate them by rule (1) to w, and since all internal edges are Hadamarded, these operators become Z. They commute through by rule (3) to the free edge of w and remain there as Z. We perform a similar transformation except that we do not commute the Z's to the free edges of inputs because these correspond to operations on inputs (i.e. logical operations) rather than operations on outputs (i.e. physical operations). Instead, we commute them through canonically to the pivot associated with that input, turning the Z back into the X as we re-associate the operator with the pivot. Finally, we commute the X through the pivot. Since the X was on an internal edge between the input and pivot, a X appears on the free edge of the pivot. The remaining X's become Z's associated with the output neighbours of the pivot and commute through to their free edges by rule (3). To reverse all these operations and achieve the identity, thereby creating a stabilizer, we apply all these operations in reverse, precisely $X(v)Z(N_o(v))X(p(i(v)))Z(N_o(p(i(v))))$. Therefore, we have proven the following theorem.

Theorem IV.2 (Inversion). Given a graph G with a feasible choice of pivots $\mathcal{P}$, the stabilizer tableau associated with the ZXCF equivalent to G is given by Eqn. (10).

From here, we can also easily write down a canonical set of logical Pauli operators for a given graph, by utilizing the same two transformation rules from above. For each input node $v_i \in \mathcal{I}$ corresponding to the ith logical qubit, construct $\overline{X}_i$ by placing $X(v_i)$, which is by definition a logical X on the ith logical qubit. To obtain the physical operator, we commute $X(v_i)$ to the (free edges of the) output nodes—here $X(v_i)$ commutes through to become $Z(N_o(v_i))$. Hence, $\overline{X}_i = Z(N_o(i))$. Similarly, $\overline{Z}_i = X(p_i)Z(N_o(p_i))$, where p_i is the pivot associated with v_i. We place a X on p_i to canonically define logical Z, but any neighbour of v_i would suffice. In this way, we have used the equivalence rules on every possible node: on $\mathcal{O}$, they create stabilizers; on $\mathcal{I}$, they create logical X; and on $\mathcal{P}$, they create logical Z.

As a consequence of our canonical logical operator construction, we observe that the degree of G controls the upper bound of the distance as well as the stabilizer weights of $\mathcal{S}(G)$.

Corollary IV.2.1. The distance of $\mathcal{S}(G)$ is at most the minimum degree of any vertex in $\mathcal{I} \cup N_o(\mathcal{I})$.

Proof. For each $v \in \mathcal{I}$, $X(v)$ is a logical operation which is equal to $Z(N_o(v))$. The weight of this operation is equal to the degree of v. Similarly, for each $v \in N_o(\mathcal{I})$, the rules of the graph tell us that applying $X(v)$ as well as applying Z to all neighbours of v does not change the circuit effected by the graph. Since v neighbours at least one input node, this means that the logical operation formed by the Paulis applied to the inputs is equal to the Paulis applied to the outputs, including v. This size of this set is equal to $|N_o(v)| + 1$, which is at most the degree of v, since v neighbours an input. The construction of these logical operations proves the desired upper bound on the distance. This also shows that the statement of the corollary could be strengthened slightly by replacing the degree of input neighbours by the number of their output neighbours plus one. □

Corollary IV.2.2. Given a graph G, define

$$\delta_{\mathcal{O}}^* = \max_{v \in \mathcal{O}} \deg(v), \quad \delta_{\mathcal{OI}}^* = \max_{v \in \mathcal{O}} |i(v)|, \quad \delta_{\mathcal{PO}}^* = \max_{v \in \mathcal{P}} |N_o(v)|. \tag{11}$$

Then $\max_{S \in \mathcal{S}(G)} |S| \le 1 + \delta_{\mathcal{O}}^* + \delta_{\mathcal{OI}}^* \delta_{\mathcal{PO}}^*$, where $|S|$ is the weight of a stabilizer S. Moreover, if every path between every pair of nodes $v, w \in \mathcal{I}$ is of length at least 3, so that every node $u \in \mathcal{O}$ is connected to at most one node in $\mathcal{I}$, then $\max_{S \in \mathcal{S}(G)} |S| \le \delta_{\mathcal{O}}^* + \delta_{\mathcal{PO}}^*$.

This result is a direct consequence of Eqn. (10).

In the next section, we will show that another important property, encoding depth, is also bounded above by the degree. We make two remarks regarding the utility of such degree bounds. First, for a general stabilizer code it is unclear as to how one may give a nontrivial upper bound on properties like distance and circuit depth. The degree allows us to algorithmically do so by compiling a stabilizer tableau into a graph and then examining the degree. Second, it is possible, at least in certain cases, to upper bound the degree itself by some function of the code parameters. We show bounds of this type in Sections V B and V C. When such a bound is possible, it provides nontrivial bounds on code properties in terms of functions of other parameters.

A. Encoding circuit with degree-bounded depth

A particularly appealing quality of the graph formalism is that it enables us to efficiently and canonically construct encoding circuits which are bounded by a small linear function of

23

the *degree* of the graph. This construction can be taken advantage of in two ways. If we already have a stabilizer code and would like to construct a nice encoding circuit, we can compile the code's tableau into a graph and then apply the procedure below. Note that Theorem IV.3 assumes a graph presentation, so if the ZXCF has local Cliffords, they are not included in the encoding circuit. They can be appended to the encoding circuit produced by the theorem, at the cost of increasing the depth by 1, since all local Cliffords are single-qubit operations. Alternatively, if we have a graph which by the previously discussed procedure represents a stabilizer code, we can directly write down this encoding circuit and have a guarantee of its depth.

Theorem IV.3. Suppose that one may initialize qubits to the $|+\rangle$ state. Given a graph G with maximum degree δ^*, there exists an efficient algorithm which outputs an encoding circuit $\mathcal{C}$ for the code with stabilizers $\mathcal{S}(G)$, such that $\text{depth}(\mathcal{C}) \leq 2\delta^* + 3$.

Proof. We construct explicitly the transformation from the graph to its encoding circuit[54]. An informal description is as follows. A graph with $|\mathcal{I}| = k$ and $|\mathcal{O} \cup \mathcal{P}| = n$ requires a circuit taking k input and $n - k$ ancillary qubits to n output qubits. We choose to send the k inputs to the k pivots on the output sides. Edges in G will generally become controlled-Z gates in the encoding circuit, with the exception of edges from $\mathcal{I}$ to $\mathcal{P}$, which become a layer of Hadamards. More precisely, construct the circuit $\mathcal{C}$ as follows.

(1) *Initialization.* Create n wires, one for each node in $\mathcal{O} \cup \mathcal{P}$. Label the output side of the wires by the node. For each wire associated to a pivot v, label the input side of the wire by the input corresponding to v. The remaining $n - k$ wires unlabeled on the input side are the ancillary qubits. Initialize these unlabeled wires to $|+\rangle$.

(2) *Input-output edges.* For each input $u \in \mathcal{I}$ and $v \in \mathcal{O}$, if $v \in o(u)$ then add a $CZ_{u,v}$ to the circuit. The order does not matter since all CZ gates commute.

(3) *Input-pivot edges.* For each input $u \in \mathcal{I}$ apply H_u. These will correspond to the edges between each input and its corresponding pivot.

(4) *Output-output edges.* For each $u \in \mathcal{O} \cup \mathcal{P}$ and $v \in N_o(u)$, apply $CZ_{u,v}$.

There are two claims to show: (a) this construction correctly yields an encoding circuit for the code described by $\mathcal{S}(G)$, and (b) $\text{depth}(\mathcal{C}) \leq 2\delta^* + 3$. The first claim is essentially a

24

direct consequence of the rules of the ZX calculus and the form of the ZXCF. Recall that G can be mapped to a ZXCF $\widetilde{G}$ by Hadamarding all edges, endowing each node with a free edge. Initially, work qubits ZX diagrams are given by Z nodes, which are the $|+\rangle$ states used in (1). As we turn the ZX diagram into a circuit, the edges which connect an input node to its corresponding node on the output side of the circuit pick up the gates between them. Since we have chosen the inputs to map to their corresponding pivot on the output side of the circuit, and the only gate between them is H, this accounts for (3) above. The remaining edges connect distinct qubits (rather than the same qubit from the input to output side), and such edges are precisely given by CZ gates. This map accounts for (2) and (4). Note that the gates are ordered in this particular way because of the causal structure of the ZX diagram. First, input edges must propagate information to the output edges, so the associated input wires must have their CZ gates to establish their interaction with the ancilla wires. Next, the circuit completes the interactions from input to output via the input-pivot Hadamards. Finally, the output edges interact, so the output-output CZ gates are placed on the ancillary wires. This completes the proof of the first claim, correctness.

To the second claim, we observe that since all CZ gates commute, the depth is given by the minimum number of groupings of CZ gates which act on disjoint sets of qubits. Such a problem reduces to finding the optimal *edge colouring* of G, i.e. the minimum number of colours needed to colour every edge, such that no two edges which share a node have the same colour. Although finding the optimal edge colouring is known to be **NP**-complete, Vizing's edge colouring theorem guarantees that the minimal colouring is at most $\delta^* + 1$, and moreover there exists an efficient algorithm which finds such a colouring [55, 56]. In sum, (2) and (4) each has depth at most $\delta^* + 1$, and (3) has depth 1, so that the total depth is at most $2\delta^* + 3$ as claimed. $\qquad\qquad\qquad\qquad\qquad\qquad\qquad\qquad\qquad\qquad\qquad\square$

Although encoding is practice is often performed by a method to prepare the logical zero state, e.g. repeatedly measuring the stabilizers until they are all $+1$, Theorem IV.3 shows that for codes that have sufficiently small degree, it may be possible to have a much stronger guarantee, namely to efficiently encode any state directly via an encoding circuit. Section V A gives an example of such an encoding circuit for a code we have constructed, and discusses how the depth may actually be substantially smaller in practice by solving small cases of minimal edge colouring. Moreover, in Section V B, we will show that the degree,

and thus the encoding circuit depth, can be bounded above by code parameters for certain families of codes. This result will thus directly upper bound the degree of the encoding circuit by code parameters.

B. Logical non-Pauli gates on graph codes

Earlier, we showed that the logical Pauli operations can be extracted immediately from the graph representation. Specifically, $\overline{X}_v$ and $\overline{Z}_v$ for $v \in \mathcal{I}$ are implemented respectively by $Z(N_o(v))$ and $X(p(v))Z(N_o(p(v)))$. We derived these logical Paulis by placing a Pauli on the free edge of a particular input node, and then applying ZX equivalence rules to push the Pauli through the node into the output.

For a completely general logical operation $\overline{U}$ and graph code G, the only algorithm to physically implement $\overline{U}$ is to unencode, apply U, and then re-encode. Such a technique is typically undesirable, since the encoding circuit is necessarily high-depth to achieve a good distance, which implies that the logical operation's implementation strongly propagates errors and therefore resists fault tolerance. Nonetheless, if the encoding circuit has a depth which is sufficiently small, it is conceivable that in some cases this generic procedure may be of use. Moreover, we already have an generically optimized encoding circuit from Section IV A, which in turn implies the following general result.

Theorem IV.4 (Generic logical operation)**.** Let G be a graph code with maximum degree δ^*, and let U be a unitary which can be implemented in depth d_U. Then there is an efficient algorithm which constructs a circuit $\mathcal{C}_U$ that logically implements U on G, such that $\mathrm{depth}(\mathcal{C}_U) \leq 4\delta^* + 6 + d_U$.

Conceivably, if a depth of δ^* is not immediately prohibitive, an additional factor of 4 significantly reduces the likelihood of practical utility. However, we will show that many important gates, including diagonal Clifford, non-diagonal Clifford, and diagonal non-Clifford gates, can be implemented generically with a reduction on the constant factor.

Theorem IV.5. For any graph code G with maximum degree δ^*, every diagonal gate U can be implemented logically on G with depth at most $2\delta^* + 5$.

Proof. The circuit is still simply the unencode-apply-reencode operation, but with cancellations due to the diagonal structure. Let E be the encoding circuit from Theorem IV.3. The circuit is of depth at most $2\delta^* + 3$ because it is of the form $CZ(V)H(V)CZ(V)$, i.e. a layer of CZ's acting on all the nodes V in the graph, a layer of H, then another layer of CZ. These respectively contribute at most $\delta^* + 1$, 1, and $\delta^* + 1$ to the encoding circuit depth. The logical operation is given by $CZ(V)H(V)CZ(V)UCZ(V)H(V)CZ(V) = CZ(V)H(V)UH(V)CZ(V)$ since U commutes with all CZ operations. This circuit has a reduced depth of $(\delta^* + 1) + (1) + (1) + (1) + (\delta^* + 1) = 2\delta^* + 5$. $\qquad\square$

As a corollary, the CZ, S, and T gates can all be generically applied with a reduction by a factor of 2 from Theorem IV.4.

For a certain non-diagonal Clifford gate, the $\sqrt{X}$ gate, we are able to even further reduce the constant to just 1. This improvement relies on a specific ZX equivalence relation involving a purely graph transformation known as a *local complementation about a vertex* (LCV). The LCV is defined for any graph and has been presented under various guises in the literature [35, 49, 51]. We have, in fact, already used the LCV in Appendix A to enforce the Clifford rule of the ZXCF. Below, we fix the vertex set V and consider different graphs which can be made with the nodes in V. Given a graph $G = (V, E)$, let $N(u) = \{v \in V : (u, v) \in E\}$ be the neighbors of $u \in V$ in G. We can assume throughout this paper that G does not permit self-edges; that is, $\forall u \in V, (u, u) \notin E$.

Definition IV.6. Let V be fixed and $G = (V, E)$ be a graph. A *local complementation about a vertex* $v \in V$ is a graph transformation LCV $: \mathcal{G} \times V \to \mathcal{G}$ given by $(V, E) \mapsto (V, E \,\Delta\, K(N(v)))$, where $K(S)$ is the edge set of a complete graph formed by nodes in $S \subseteq V$.

Intuitively, a LC about a vertex v can be described as follows. Consider the edges of the complete graph built from $N(v)$, and then toggle all these edges in v. That is, if $e \in E \cap K(N(v))$, then remove e from E, and if $e \in K(N(v)) \setminus E$, add e to E.

The LCV builds a bridge between unitary operations on graph codes and inherent graph transformations. Suppose we have a graph $G = (\mathcal{I} \cup \mathcal{P} \cup \mathcal{O}, E)$ and we wish to apply a logical unitary $\overline{U}$; that is, $\overline{U}_v$ for $v \in \mathcal{I}$. Generically, if we attempt to use the ZX equivalence rules to push $\overline{U}_v$ to the output, the rules will add more local operators and change edges,

27

resulting in $\overline{U}$ applied to the output $\mathcal{O}$ of a *different graph*, which corresponds to a different code. To make this distinction clearer, let $U_v(G)$ be the operator U applied to $v \in V$ on G. If $v \in \mathcal{I}$, then $U_v(G)$ is a logical operator; otherwise, $U_v(G)$ is a physical operator. For brevity, if $U = U^{(1)} \dots U^{(m)}$, we denote $U_v(G) = U^{(1)} \dots U_v^{(m)}(G)$. We also denote $U_{v_1}(G) \otimes \dots \otimes U_{v_m}(G) = U_{\{v_1, \dots, v_m\}}(G)$.

The specific connection between the LCV and the $\sqrt{X} = HSH$ gate is given by the following standard ZX equivalence relation, whose proof can be found in Refs. [35, 49, 51].

Claim IV.7. Let $G = (V, E)$ be a graph. Then $\sqrt{X}_u(G) = HSH_u(G) = S_{N(u)}(\text{LCV}(G, u))$.

Therefore, in order to apply a logical $\sqrt{X}$ on some $u \in \mathcal{I}$, we apply the LCV about u, and then apply a S gate on all nodes in $N(u)$. Since $N(u) \subseteq \mathcal{O} \cup \mathcal{P}$, all the S gates are physical.

Lemma IV.8. Given a graph G representing a code, the graph transformation $\text{LCV}(G, u)$ for $u \in \mathcal{I}$ can be implemented with a quantum circuit of depth at most $\deg(u)$. There is an efficient algorithm outputting this circuit.

Proof. $\text{LCV}(G, u)$ is implemented by CZ_{vw} for all $(v, w) \in K(N(u))$. Since $|N(u)| = \deg(u)$, each node in $K(N(u))$ has degree $\deg(u) - 1$. By Vizing's theorem, there is an efficient algorithm to arrange the CZ gates to have depth at most $(\deg(u) - 1) + 1 = \deg(u)$. $\square$

Theorem IV.9. Let G be a graph. There is an efficient algorithm which finds a circuit that implements the logical $\sqrt{X} = HSH$ gate on an input node u with depth at most $\deg(u) + 1$.

The proof is a direct consequence of Claim IV.7 and Lemma IV.8.

In general, we do not see a way to completely reduce the implementation depth of an arbitrary Clifford circuit because the Hadamard gate does not appear amenable to further optimization. To have a complete set of Clifford operations which can be implemented in depth strictly better than that of Theorem IV.4, one solution is to start with a self-dual CSS code, which admits a transversal Hadamard. In this case, the local complementation simplifications that push a H gate through to the output will cancel out in just the precise way as to produce H's on all output nodes while preserve the graph structure. $\{H, \sqrt{X}, CZ\}$ is a generating set of the Clifford group, and thus the above results imply that any self-dual CSS code implements logical Cliffords at a depth that is reduced by at least a factor of 2 from the generic procedure of Theorem IV.4.

C. Game unification of stabilizer coding algorithms

Thus far, given a graph, we have described its corresponding stabilizers, given a set of logical operators, and provided a simple upper bound on the distance. To complete our fully graph formalism of stabilizer codes, we will show that important code algorithms— distance calculation or approximation, stabilizer weight reduction, and decoding—can all be expressed in a unified graph manner, namely by a single class of one-player games on the graph.

Definition IV.10 (Quantum lights out). An instance of a quantum lights out (QLO) game [57] on a graph G is described as follows. The notion of a free edge is not needed for QLO and will be discarded. Every node is endowed with both a light and a switch, both of which are binary (i.e. on of off), which are initially off. Flipping a switch at node v (a) permanently destroys the light at v if $v \notin \mathcal{I}$ and (b) toggles all intact (i.e. non-destroyed) lights on the neighbours of v. Let Alice be the player. The graph begins with some initial configuration of lights. The game consists of two rounds:

(1) Depending on the instance, Alice may be allowed to flip switches in the input.

(2) Alice chooses a set of n nodes $v_1, \ldots, v_n \in \mathcal{P} \cup \mathcal{O}$, subject to some some instance-dependent constraints. For each node v_i, in order, Alice chooses whether to toggle the switch at v_i or only to destroy the light on v_i. The game ends when the lights reach an instance-specific desired final configuration, usually with all non-input lights off or destroyed.

The specific instance of the QLO game specifies the initial light configuration, whether round (1) exists, the constraints in round (2), and the desired final configuration, e.g. all lights are turned off. Regardless of instance, Alice must make at least one move in round (2). We say that Alice wins in n moves if she makes n choices that lead to the desired final configuration of the game.

By correctly choosing the instance of the game, we can represent many important stabilizer coding algorithms as strategies for QLO games. We begin by showing that finding the distance of a code is QLO. Note that the distance is invariant under unitaries on inputs, and hence every equivalent Clifford encoder has the same distance.

Theorem IV.11 (Distance is QLO). Given a graph G, denote the distance of the code represented by $d(G)$. $d(G)$ is calculated by the following QLO instance. Initially, all lights are off. In round (1), Alice may flip any number s of switches in $\mathcal{I}$. In round (2), Alice has no constraints and may flip any non-input switch or destroy any non-input light. The final configuration consists of all non-input lights off or destroyed, and either at least one input light is on, or $s \geq 1$. Under this instance,

$$d(G) = \min_{\mathcal{A}} m_{\mathrm{D}}(\mathcal{A}, G), \tag{12}$$

where $\mathcal{A}$ is Alice's strategy and $m_{\mathrm{D}}(\mathcal{A}, G)$ is the number of moves she made in round 2. As a consequence, every distance approximation algorithm on G to multiplicative error ϵ is a ϵ-approximately optimal strategy in the distance QLO game instance.

Proof. Each of the switches flipped in the ith input corresponds to $\overline{X}_i$, i.e. logical X on logical qubit i. If the game allowed for flipping a single light at a node, this would correspond to applying a Z on the node. There is no point to applying a Z operator multiple times to the same output node, as they will cancel (and we can order them so that no phase occurs). Hence, instead we simplify by destroying the light altogether as a reminder that re-toggling this light does not increase an operator's weight. Next, toggling lights on all neighbours of a node v correspond to applying $X(v)$. There is no additional Pauli weight if we apply both $X(v)$ and $Z(v)$, so for convenience we also destroy the light on v when we flip the switch. In sum, destroying lights and flipping switches correspond to physical Z and X operators. Lights turned on at inputs after all lights on outputs have been extinguished are logical Z operators. Consequently, the entire distance QLO game consists of applying some logical X operators and translating them into physical operators and logical Z operators. In other words, the physical operator represented by the n moves apply the logical product of the initial logical X's and the final logical Z's, which is a nontrivial logical operator if at least one of the two is not vacuous, i.e. if at least one input light is left on or $s \geq 1$. Since each move increases the physical operator's weight by exactly 1, the minimum number of moves is precisely the distance. $\square$

Since finding the distance of a stabilizer code is **NP**-complete [58], we may immediately conclude that optimally playing QLO on arbitrary graphs is also **NP**-complete.

Theorem IV.12 (Weight reduction is QLO). Let $\{S_i\}$ be the canonical stabilizer generators of G. Without loss of generality, fix S_1 the first stabilizer. Then the minimum-weight stabilizer S'_1 which can replace S_1 in the tableau, i.e. remains independent of $S_1, \ldots, S_{n-k}$ is given by a QLO game instance. Initially, all lights are off. There is no round (1). In round (2), Alice may freely flip switches on any node except v_1, the switch in $\mathcal{O}$ corresponding to S_1. She must flip the switch at v_1 *exactly once*. The final configuration consists of all lights destroyed or off. Under this game instance,

$$|S'_1| = \min_{\mathcal{A}} m_{\mathrm{WR}}(\mathcal{A}, G), \tag{13}$$

where $\mathcal{A}$ is Alice's strategy and $m_{\mathrm{WR}}(\mathcal{A}, G)$ is the number of moves she made in round 2. Thus the minimum weight is equal to the minimum number of moves to end the game.

We formulate the weight reduction theorem in terms of the canonical stabilizers in the graph representation. We observe that an analogous result applies for a different set of stabilizers, so long as they are independent.

Proof. Initially, we apply $X(v_1)$. The canonical stabilizer represents the trivial strategy of flipping pivot switches to remove lights from inputs, and then destroying all remaining lights. However, any sequence of moves that turns all lights off, i.e. effectively applies the identity on the graph, is also a stabilizer. Because we restrict Alice from flipping the switch at v_1, the resultant stabilizer is both nontrivial (i.e. not the identity) and independent from all other S_i, since S'_1 is still the only stabilizer at $X(v_1)$. Hence, the minimum number of moves, plus one for $X(v_1)$, represents the new weight as claimed. $\qquad\square$

By examining the proof, we also observe that the act of writing down the canonical stabilizers and the canonical logical operators are also instances of substantially simpler QLO instances.

Theorem IV.13 (Decoding is QLO). Suppose that after application of a noisy channel to the codeword, we measure the canonical (or more generally, any known set of) stabilizer generators of a graph G. We thereby obtain syndrome bits $s_1, \ldots, s_{n-k} \in \{\pm 1\}$. Then, the recovery map that should be applied is given by a QLO game instance. Initially, the light at each vertex $v_i \in \mathcal{O}$ corresponding to stabilizer S_i is turned on if $s_i = -1$. All remaining lights start off. In round (1), Alice may flip any number of switches in $\mathcal{I}$. In round (2), Alice

has no constraints aside from only being able to act on nodes in $\mathcal{O} \cup \mathcal{P}$, as usual. The final configuration consists of all non-input lights off or destroyed. Under this instance,

$$r(S, G) = \min_{\mathcal{A}} m_{\mathrm{DC}}(\mathcal{A}, S, G), \tag{14}$$

where S is the set of syndromes, r is the number of moves in the optimal recovery map, $\mathcal{A}$ is Alice's strategy and $m_{\mathrm{DC}}(\mathcal{A}, S, G)$ is the number of moves she made in round (2). We note that input lights being on does not affect anything in round (2) or in the minimization condition. This means that, where convenient, input lights can be completely ignored.

Proof. We show that at each step of the decoding procedure, the current syndromes s_i (corresponding to v_i) are given by $(-1)^{\eta_i}$, where η_i is the parity of the number of lights that are currently on in certain sets $\mathcal{T}_i := \{v_i\} \cup p(i(v_i))$. We proceed by casework on each possible type of error, and the stabilizers that they affect.

(1) $E = Z(v)$ for $v \in \mathcal{O}$. E anticommutes with stabilizers which contain $X(v)$. The unique canonical generator which contains $X(v)$ is $S(v)$. Thus, applying a Z to a node in $\mathcal{O}$ toggles its light.

(2) $E = Z(v)$ for $v \in \mathcal{P}$. E anticommutes with stabilizers which contain $X(v)$. These are the stabilizers associated with the *non-pivot output neighbours* of the *input* associated with v, i.e. $S(w)$ for all $w \in o(i(v))$. Applying a Z to a node in $v \in \mathcal{P}$ negates the syndromes of *all* stabilizers of the vertices $o(i(v))$, and therefore toggles all lights in $o(i(v))$. We can either view the action of the Z as toggling the lights $o(i(v))$ or, equivalently, as just toggling the light at v, since this will also negate all of the desired syndromes. The reason for this is that $v \in \mathcal{T}_i$ for all v_i in $o(i(v))$. Toggling the lights $o(i(v)) \cup \{v\}$ can be done in round (1) by toggling the switch at $i(v)$, so this equivalence is justified. This means that toggling the light at v is equivalent to toggling the lights of $o(i(v))$. Thus, applying a Z to a node in $\mathcal{P}$ toggles its light.

(3) $E = X(v)$ on any $v \in \mathcal{O} \cup \mathcal{P}$. E anticommutes with stabilizers which contain $Z(v)$. These are $S(w)$ for $w \in o(v)$ as well as $w \in o(i(p(v)))$ due to the presence of Z's in $S(w)$ on $o(p(i(w)))$ (note that the order of i and p is backwards when we consider stabilizers affected by a node). Applying an X to a node $v \in \mathcal{O} \cup \mathcal{P}$ toggles all

32

lights in $o(v) \, \Delta \, o(i(p(v)))$, or equivalently, $o(v) \cup p(v)$. As shown previously, $X(v)$ is equivalent to Z on all neighbours of v, some of which may be pivots. Applying an X to v flips the switch at v, and thereby toggles the lights on $N_o(v)$, its pivot and output neighbours. This is equivalent to toggling the lights $o(v)$ and then toggling $o(i(p(v)))$. Thus, applying an X to a node in $\mathcal{O} \cup \mathcal{P}$ toggles all neighbouring lights.

A decoding procedure involves turning off lights by acting on nodes in $\mathcal{O} \cup \mathcal{P}$ (corresponding to physical recovery operators), using the fewest number of moves possible. For $v \in \mathcal{O}$, let $S(v)$ be the canonical stabilizer associated with v. The moves in round (1) do not change the syndromes, since for any stabilizer S_i, toggling any input switch will necessarily toggle either zero or two lights in $\mathcal{T}_i = \{v_i\} \cup p(i(v_i))$, depending on whether or not the input neighbours v_i. Additionally, we note that breaking a light at a node after applying the switch at that node represents ambivalence between applying an X or a Y, but if Alice is interested in finding the proper recovery map instead of just the map's size, she should leave all lights unbroken. Then, when she is done toggling switches, she can choose to turn off any lights at vertices whose switches she toggled without having this count as a move in round (2). We conclude that decoding algorithms are QLO strategies. $\qquad\square$

We note that construction of the recovery map is very closely related to the calculation of the distance.

The unified expression of all three algorithms, combined with the many complex techniques to perform optimizations on graphs that have been developed in past decades, suggest that the study of approximating optimal QLO strategies may be a promising pathway for devising coding algorithms.

V. APPLICATIONS OF THE GRAPH FORMALISM

We proceed to provide constructive evidence in three areas for the utility of a graph representation. First, in Section V A, we argue that for near-term experimental purposes, the graph formalism provides a simple and flexible prescription for the design of codes with a desired rate R and distance d. Intuitively, this advantage occurs because we can appeal to the geometrical and topological structure of graphs, as well as take inspiration from well-studied graphs, to get close to a distance d. We then describe improved results for random

codes and construct an efficient graph decoder for a family of stabilizer codes constructed from graphs.

A. Flexible code design

Generally, stabilizer tableaus have proven more useful as a description rather than a constructive mechanism. Most well-known stabilizer codes constructed are actually CSS codes [25, 27, 28, 34], and non-CSS stabilizer codes are usually found by some alternate presentation. The lack of use of stabilizer tableaus is not unusual, as it is simply not obvious as to what collections of Pauli strings construct codes with high distance, easy decoding, gates, geometric properties etc. The universality of the graph representation of stabilizer codes, combined with a rich history of graphs in error correction [26, 28, 38, 59], suggests that a promising technique to construct certain codes lies in finding sufficiently "nice" graphs.

Because of its universal expressive power, the graph representation in this work has parameters that scale with distance. As we showed previously, the distance is bounded above by degree parameters of the graph, and the canonical stabilizers have weights that also scale with the degree. Therefore, the graph representation is best suited for finding codes with a desired approximate numerical values of code parameters, as opposed to asymptotically good LDPC codes. In other words, graphs provide a flexible technique to generate potentially practical small-scale codes.

As an example of this flexibility, if one wanted to create a code with a particular distance, one can set the degree of the graph in accordance with Corollary IV.2.1. On graphs that do not have large overlaps in sets of neighbours, the distance will be determined by the degree of the input vertices as well as the output-degrees of input neighbours. Achieving a certain rate translates to having a sufficiently high density of inputs, which in turn can influence the required degree of the input neighbours. Some experimental devices or algorithms may benefit from codes that have at most a particular number of physical qubits or encode a minimum number of logical qubits, both of which are easy to set in the graph formalism. If ensuring that the physical qubits behave similarly in a highly uniform manner, a graph could be chosen to be highly regular and symmetric, such as the 5-, 7-, and 9-qubit codes from Section III. Further still, a graph can be chosen to be planar and local in two dimensions,

or perhaps supporting only a fixed number of long-range connections for ease of practical implementation. On the other hand, a graph embedded into a higher-dimensional space, such as a high-dimensional grid graph for example, could be easier to represent or simulate classically. We will give examples of codes with each of these properties below.

The distance calculations of codes in this section were performed by direct computation. The code is freely available for use [60].
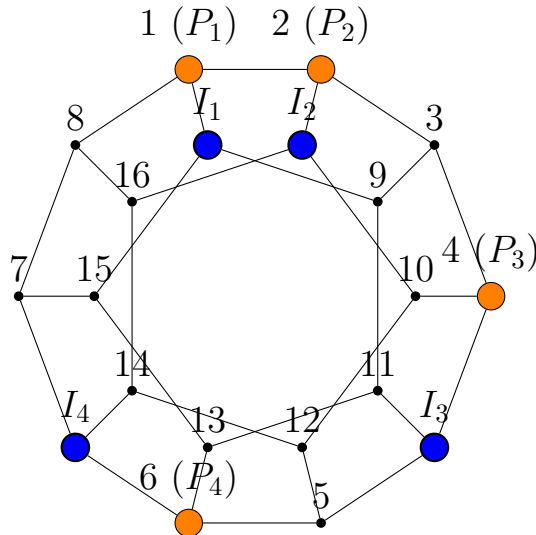

FIG. 6. The $[\![16, 4, 3]\!]$ dodecahedral code. Blue nodes are inputs, black nodes are outputs, and orange nodes are pivots. This code is the optimal packing of input nodes into the dodecahedral graph so that no inputs have a path between them of length less than 3. As the dodecahedron has odd cycles, it is not a bipartite graph and therefore this code is a non-CSS stabilizer code. The rate of the code is higher than that of the 5-qubit code, making it the best small non-CSS code the authors are aware of. The labels indicate an ordering of the input and output nodes as well as the pivots (lowest numbered nodes next to each input). There are no extra input-pivot edges but we allow pivot-pivot edges where this does not change our constructions. An ordering can be chosen on the nodes to avoid all pivot-pivot edges.

1. The dodecahedral code

We now showcase a few examples of novel small codes that we constructed from the graph formalism. As a first example, we examine the 7-qubit Steane code in Fig. 3, which

takes the shape of a cube. Such a geometric structure motivates the exploration of other highly regular geometric solids as graph codes, such as the platonic solids. While the graphs of a tetrahedron and octahedron perform rather poorly as codes due to their particular symmetries, the graph of a dodecahedron represents a relatively good code. Figure 6 exhibits the dodecahedral code, which has parameters $[\![16, 4, 3]\!]$. Since the degree of every node is 3, the dodecahedral code saturates its distance-degree bound. The rate has also been optimized while not compromising the distance. To maintain a distance equal to the degree, no two inputs may share a neighbour (as otherwise there exists a logical operator of lower weight), so the maximum number of inputs that can be selected is 4. We remark that this graph is not a CSS code, being non-bipartite, but has rate $1/4$. As such, it is strictly better than perhaps the most well-known non-CSS stabilizer code, the $[\![5, 1, 3]\!]$ 5-qubit code from Section III.
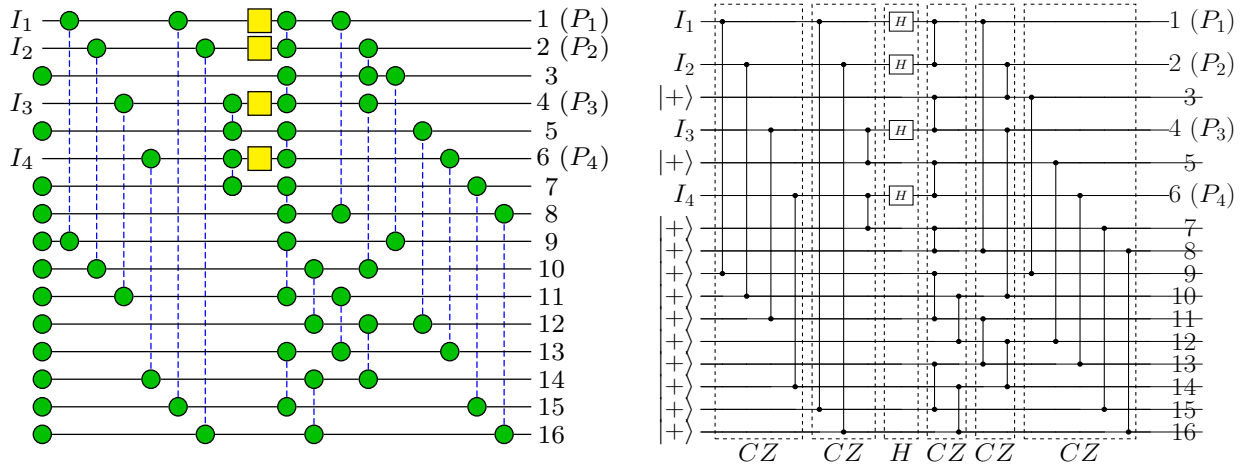

FIG. 7. Two presentations of the encoding circuit of the dodecahedral code, labeled as in Fig. 6. On the left, the presentation is of a ZX diagram. Yellow boxes indicate H gates and blue dashed edges are, as usual, Hadamarded. On the right, the presentation is of a standard quantum circuit. Each dashed block represents a set of transversal (depth-1) operations, so that the circuit depth is the number of blocks, in this case 6. The presentation here is partially optimized, by inspection, to improve upon the upper bound given in Theorem IV.3. It is possible with further heuristics to produce a depth-5 (but more visually complicated) circuit, which is provably optimal.

To complete our discussion of the dodecahedral code, we apply Theorem IV.3 to give the code a low-depth encoding circuit. Figure 7 illustrates two representations of the encoding circuit. On the left, we draw a ZX diagram which appears as an intermediate step in the

algorithmic construction in Theorem IV.3. On the right, we translate the ZX diagram into standard quantum circuit notation. The translation is an immediate consequence of the ZX calculus rules: a Z node with a single output is a $|+\rangle$ state and a Hadamarded edge between two Z nodes implements a CZ gate. Corresponding to the theorem, the CZ gates before the layer of Hadamards form the input-output edges; the Hadamards effectively form input-pivot edges; and the CZ gates after the layer of Hadamards form the edges from non-inputs to non-inputs. We observe also that the application of the ZX calculus simplification rules to the diagram in Fig. 7, such as merging Z nodes together, recovers the graph representation of the dodecahedral code itself. In this sense the encoding circuit appears almost immediately from the graph representation.

While our results about the worst-case encoder depth suggest that it may have a depth of up to 9, we have applied some heuristic, "by-inspection" analysis to by hand further optimize the depth to 6. Further compilation of this circuit would allow us to reduce the depth further. This is because output-output edges commute with every gate in the circuit as they are not on the input-pivot wires containing the only non-diagonal gates. In particular, the 5 gates in the last block can be moved to the second, first, fourth, first, and first blocks, respectively, resulting in a circuit of depth 5. This is the minimum possible depth as that is the number of gates acting on some qubits, such as the first input.

2. Covering spaces and the 5-covered icosahedral code

We next consider a code based on the graph of an icosahedron. Since the vertices have an icosahedron have degree 5, we can hope that a code based on this graph would have distance 5. Unfortunately, we find that the code underperforms the degree bound because a Y gate on two antipodal vertices is equivalent to applying a Z to each vertex. Hence, a logical Y on any input is a logical operation of weight 3, with one Y on the vertex opposite the input and two more on any two antipodal vertices. This observation also implies that if we wish to add more than one input to the icosahedron, our distance will be reduced further, as a logical operation would just consist of Y's on two vertices opposite the inputs. To get around this issue, we lift the graph into a finite covering space. Specifically, we can imagine taking a double cover of the icosahedron by "puncturing" the icosahedron in the center of two
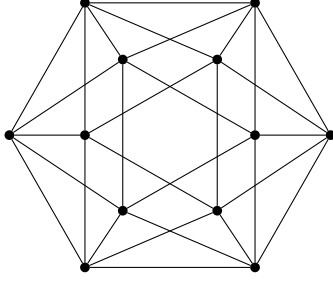
FIG. 8. The graph of an icosahedron. Although it has degree 5, marking a single node as an input only creates a code of distance 3. We can puncture the icosahedron through the two central faces and take the double cover of this icosahedron with the index of a vertex matching the winding number of a path around the puncturing axis. If we select one of the 6 "outer" nodes, nodes that are not vertices of the punctured faces, and mark both copies of the selected nodes as inputs, we create a $[\![22, 2, 5]\!]$ code. We can improve the rate by covering the icosahedron 5 times and selecting nodes along the perimeter, each rotated 300° around the puncturing axis from the last. Since we mark one node every 300°, we create 6 input nodes, because $6 \cdot 300° = 5 \cdot 360°$. The 5-covered icosahedral code has parameters $[\![54, 6, 5]\!]$.

opposite faces and attaching a winding number to each vertex, which is computed modulo 2. In doing so, we find that the double-covered graph with a single input has distance 5. In fact, we can improve the rate slightly by taking an n-cover of the icosahedron. Specifically, when $n = 5$, we can fit 6 input vertices, where the inputs are not vertices of the punctured faces, and each of which is wound 300° around from the previous input. In Fig. 8, if we puncture the two central faces, the inputs in the 5 copies of the icosahedron will be on copies of the 6 vertices along the perimeter, each rotated 300° from the last. This construction creates a $[\![54, 6, 5]\!]$ code.

The ideas used to create the five-covered icosahedron can be extended more generally to extend otherwise finite graphs. In fact, arbitrarily complicated covers can be proposed, leading all the way up to the universal cover of the graph. If regularity and a finite set of vertices are desired, some periodic boundary conditions can be established to keep the graph finite. In general, such covering space graphs may provide a promising path towards code design recipes in this framework. In the case of Cayley graphs, similar ideas have already been utilized to construct quantum LDPC codes from Cayley graphs of free groups with

generators comprised of columns of a classical parity check matrix [61].

3.   Planar and higher-dimensional lattice-type codes

Even more generally, lattice-type codes enable the construction of families of codes with increasing degree (and thus, potentially, increasing distance) while also preserving some notions of regularity that are often desirable in code construction. If we wish to remain in two dimensions and also have a Euclidean lattice, we are restricted in the sense that the triangular lattice, which has degree 6, is the highest-degree such lattice. We numerically confirmed that such lattices do yield distance-6 codes. Beyond degree 6, we can either raise the dimension or embed graphs in non-Euclidean spaces. For example, an embedding of triangular surfaces into hyperbolic spaces yields the Poincaré's disk map. However, because the Poincaré disc packs infinitely many points into a finite space, we would have to construct finite approximations and then study the effect of artificially establishing a finite boundary. Analysis of such effects appears difficult and is out of the scope of this work. Nonetheless, such classes of codes in non-Euclidean spaces may prove useful, and even connected to HaPPY codes [62], which also use graphs in hyperbolic space.

The other path—increasing the dimension—is more amenable to analysis. A simple, general recipe to construct a code from a lattice is to cut off the lattice in each dimension at a finite number of intervals, endow the finite version with periodic boundary conditions in each direction, and then embed some inputs and pivots within them such that the choices of pivots are valid and inputs are not connected.

One immediate advantage of this approach is a robustness to deformation that does not hold for CSS codes. In particular, we showed in Observation II.5 that a graph code is CSS if and only if it is bipartite. For lattices with periodic boundary conditions, the bipartite condition is equivalent to the length of every single dimension of the torus being even. Such a requirement is very non-local and does not change the central architecture of the code. Even for CSS torii, the addition of one vertex far from any inputs such that it forms an odd-length cycle will make the code no longer CSS but will not meaningfully affect any of the code's parameters.

When constructing families of codes in the graph formalism, it is important to consider

the geometry of the graph as well as the placement of the inputs. To make use of the graph formalism for computing stabilizers and logical operations, the identification of pivot nodes is paramount. While the ZXCF does not allow pivot-pivot edges, these do not affect the expressions of the graph formalism. Thus, for easy pivot selection, it suffices for all of the inputs to be separated by paths of length at least 3 from each other in the graph. Although such a restriction is not necessary for code construction, it does allow for any input's neighbour to be chosen as its pivot as that node would necessarily not border any other inputs by the distance condition. The downside to such graphs, however is that their rate is bounded as $R \leq \frac{1}{d}$, where d is the degree of the graph (assuming it is regular). In other words, they have a strong rate-distance tradeoff. Nonetheless, such graphs may be interesting at small scales, as we have already seen.

In higher dimensions, perhaps the simplest lattice we can utilize to build a code is the boolean hypercube in an arbitrary m dimensions. We represent the hypercube by labeling nodes as length-m bitstrings and connecting two nodes if their Hamming distance is exactly 1, i.e. they differ by one bit flip. We observe immediately that the hypercube code is CSS for all m, since the hypercube is bipartite. To select inputs, we observe that if we wish to place inputs such that they are separated by paths of length at least 3, we can leverage classical coding theory to provide this guarantee automatically. Specifically, we consider the *classical* $[2^r - 1, 2^r - r - 1, 3]$ Hamming codes [63]. Letting $m = 2^r - 1$, we can equivalently express the parameters as $[m, m - \log(m + 1), 3]$, where the code is perfect when m is one less than a power of 2. Note that all logarithms in this paper are taken to be base 2. Since this code has $m - \log(m + 1)$ logical bits, there are a total of $\frac{2^m}{m+1}$ codewords represented as length-m bitstrings. Because the Hamming code's distance is 3, all such codewords are guaranteed to have a separation in the hypercube by paths of length at least 3. Therefore, by choosing the input nodes in the m-dimensional hypercube to be those whose bitstring is a codeword in the $[m, m - \log(m + 1), 3]$ Hamming code, we obtain a code with $\frac{2^m}{m+1}$ logical qubits, $2^m - \frac{2^m}{m+1} = \frac{m2^m}{m+1}$ physical qubits, and a distance D_m bounded above by the degree m. That is, a $[[\frac{m2^m}{m+1}, \frac{2^m}{m+1}, D_m]]$ family of codes. Due to the length-3 separation of inputs, any choice of pivots uniquely connected to a corresponding input will do; later, we will show that it is both possible and particularly convenient to choose the pivots such that they are also separated by paths of length at least 3. We will also later prove in Section V B that

40

$D_m \gtrsim m/2$, up to an additive error of 2, and give evidence that $D_m = m$. For example, for $m = 7$, the code is $[\![112, 16]\!]$ with distance between 4 and 7. Asymptotically, the code scales as $[\![n, \Theta(\frac{n}{\log n}), \Theta(\log n)]\!]$.

To improve the rate further without the strong distance-rate tradeoff barrier $R \leq \frac{1}{d}$, we will need to use the most general form of graph codes, namely those with inputs separated by paths of length 2. We conclude this section with some remarks on how such codes may be constructed. In a grid lattice on a m-dimensional torus, we wish to pack inputs more closely while being mindful of the fact that our distance will be bounded above by the number of output nodes next to each output node. One such construction is as follows. First, consider a foliation of the m-torus into sequentially numbered "layers" of $(m - 1)$-dimensional toric hypersurfaces that together stack into a m-dimensional torus. In each layer, we will consider sets of vertices grouped by their *index*, the sum of their integer coordinates taken mod 3. We can assume that the size of each torus dimension is a multiple of 3 to make sure these sets are well-defined. Note that the index does not consider the mth coordinate, as that is determined by the number of the layer that a node ends up in.

(1)   In layer 1, we set all nodes of index 0 to be inputs, with pivots in layer 2.

(2)   In layer 2, we set all nodes of index 0 or 1 to be pivots.

(3)   In layer 3, we set all nodes of index 1 to be inputs, with pivots in layer 2.

(4)   We repeat this 3-layer structure as many times as desired.

Such a pattern is essentially a 3-layered, high-dimensional analog of a checkerboard pattern. Again, we see that our distance upper bound is d, as vertices such as those of index 1 in layer 1 have d inputs among their $2d$ neighbours. More sophisticated techniques are necessary, however, to lower-bound the distance. However, the rate of this code is a constant $\frac{2}{7}$, which is achieved at any scale of this code, without the need for extreme numbers of qubits for the asymptotic behaviour of the code parameters to be expressed. Additionally, we note that if an odd number of 3-layer structures are used or if any of the dimensions of each layer is odd, the code graph will have a cycle of odd length, meaning that the resulting code will not be a CSS code.

These examples showcase a wide variety of families and constructions, both small and large, that can be achieved with the graph formalism. While some are sufficiently small to admit brute-force computational distance calculations, others are more difficult to analyze and will require additional distance-bounding tools to understand. We take a first step in this direction in the next section.

B. Decoding algorithms and analysis

We continue our discussion by constructing a simple greedy decoding algorithm on graphs. We give a sufficient-condition characterization of graphs for which the greedy decoder successfully recovers errors up to half of the theoretical maximum. That is, graphs which satisfy this certain property have a provable distance *lower bound* based on its degree. Finally, we will show that the $[\![\frac{m2^m}{m+1}, \frac{2^m}{m+1}]\!]$ boolean hypercube code, defined in Section V A, satisfies this characteristic and thus is efficiently decodable.

Denote for simplicity $oip(v) := o(i(p(v)))$ and $oi(v) = o(i(v))$. In Theorem IV.13, we showed that decoding amounts to strategies in QLO. There, we presented a more sophisticated approach in which the lights on pivots encoded information about stabilizers that were connected to the pivots' corresponding inputs. In our greedy decoder, it will be simpler for analysis purposes to do away with this notion and decode more directly. That is, X errors on a node v toggle lights in $o(v) \Delta oip(v)$, Z errors on a pivot v toggle lights in $oi(v)$, and Z errors on a non-pivot output v toggle the light at v. (Y errors are treated as both an X and a Z error.) As a consequence, there are no lights at all on pivots (since there are no stabilizers there). Moreover, we apply recoveries by directly performing the same operations, e.g. if we wish to do a X-recovery on a node v, we toggle lights in $o(v) \Delta oip(v)$ and destroy the light at v. We note that this paradigm is equivalent to the QLO game instance from Theorem IV.13. In particular, suppose that after every switch flip on v Alice also flips the switches on $ip(v)$, which immediately toggles the lights on the neighbours, i.e. turning off the lights in $p(v)$ and turning on the lights in $oip(v)$. This rule maps the QLO game in the theorem to the setup we have given here. But the flipping of input switches can be moved post-hoc to round (1) in the game, not changing the number of moves made in round (2), and thus the two paradigms are entirely equivalent.

42

Algorithm 1: Greedy graph decoder

Function GreedyDecoder(G):

    $explored \leftarrow []$, $(v_0, n_0) \leftarrow (\text{nil}, 0)$

    while *True* **do** // X error recovery loop

        for $v \in \mathcal{O} \cup \mathcal{P}$ **do**

            $\text{gap} \leftarrow 2\texttt{NumLights}(o(v)) - |o(v)|$

            // If more than half of lights around v are on, 'gap' is

                positive

            if $gap > n_0$ **then**

                $v_0 = v$, $n_0 = \text{gap}$

        if $v_0 \in explored$ **or** $gap = 0$ **then**

            break

        $\texttt{Recover}_X(v_0)$ // toggle lights at $o(v_0) \, \Delta \, oip(v_0)$, destroy light at v_0

        Append v_0 **to** explored

    $explored \leftarrow []$, $(v_0, n_0) \leftarrow (\text{nil}, 0)$ // Reset tracking variables

    while *True* **do** // Z error *on pivots* recovery loop

        for $v \in \mathcal{P}$ **do**

            $\text{gap} \leftarrow 2\texttt{NumLights}(oi(v)) - |oi(v)|$

            if $gap > n_0$ **then**

                $v_0 = v$, $n_0 = \text{gap}$

        if $v_0 \in explored$ **or** $gap = 0$ **then**

            break

         $\texttt{Recover}_Z(v_0)$ // toggle lights at $oi(v_0)$

        Append v_0 **to** explored

    for $v \in \mathcal{O}$ **do** // Z error *on outputs* recovery loop

        if $LightIsOn(v)$ **then**

            $\texttt{Recover}_Z(v)$ // Destroy light at v

    return

The greedy decoder is a strategy in the decoding instance of QLO. In particular, the operations permitted are $\texttt{Recover}_X$ and $\texttt{Recover}_Z$, which flip switches or destroy lights depending on the node v chosen. We showed earlier in Theorem IV.13 how a QLO strategy

maps to a physical recovery operation. The construction of the algorithm is based on the following intuition. If $v \in \mathcal{O}$ suffers a X error, the stabilizers at $o(v) \,\Delta\, oip(v)$ will measure -1, so in the QLO game the lights in $o(v) \,\Delta\, oip(v)$ will turn on. Perhaps there will be some Z errors in $o(v) \subseteq \mathcal{O}$, each of which correspond to turning on a single light in $o(v)$. Therefore, assuming it is difficult to turn on more than half of the lights in $o(v)$, a good guess is that if more than half of the lights are on in $o(v)$ then v has suffered an X error, at which point we can apply X on v to reverse the error, via $\texttt{Recover}_X$. Note that we do not consider the status of the lights in $oip(v)$ when deciding whether to toggle v, as all lights in $oip(v)$ can be toggled by applying an X to any neighbour of $p(v)$. The recovery may itself turn on more lights in other places, so to avoid issues related to parallelism, we work in sequence and apply X recoveries one at a time, in order of nodes which have the most neighbours with lights on. A similar story holds for Z errors on $v \in \mathcal{P}$. They are detected by stabilizers in $oi(v)$, so we apply the analogous greedy recovery operation there. Finally, for remaining lights on in $v \in \mathcal{O}$, we directly destroy the lights with Z operations.

The key property within this intuition that seems to enable greedy-type decoding is the idea that it must be difficult to "fake" an X error on some v by using a small amount of moves to turn on most of the lights in $o(v)$. We now formalize this property to give a simple performance guarantee of the greedy decoder.

In this definition, we are specifically interested in how many lights an operation at node v can toggle in the set $o(u)$, the set we examine to determine whether to toggle the switch at u.

Definition V.1. Let $G = (V, \{o, i, p\})$ be a graph with input, output, and valid pivot nodes. We say that G is *B-sensitive* if

(a) for all $u \in \mathcal{O} \cup \mathcal{P}$, $v \in \mathcal{O} \cup \mathcal{P}$, $u \neq v$, $|o(u) \cap (o(v) \,\Delta\, oip(v))| \leq B$ (X error on any output or pivot v),

(b) for all $u \in \mathcal{O} \cup \mathcal{P}$, $v \in \mathcal{O}$, $u \neq v$, $|o(u) \cap (\{v\} \,\Delta\, o(v) \,\Delta\, oip(v))| \leq B$ (Y error on non-pivot output v),

(c) for all $u \in \mathcal{O} \cup \mathcal{P}$, $v \in \mathcal{P}$, $u \neq v$, $|o(u) \cap (oi(v) \,\Delta\, o(v) \,\Delta\, oip(v))| \leq B$ (Y error on pivot v),

(d) for all $u \in \mathcal{I}$, $v \in \mathcal{P}$, if $u \neq i(v)$, i.e. v is not the pivot corresponding to input u, then

  $|o(u) \cap oi(v)| \leq B$ (Z error on pivot v) .

The case $|o(u) \cap \{v\}| \leq B$ (Z error on non-pivot output v) is not included because it is always satisfied, since $B \geq 1$.

These four conditions together form a sufficient condition to place a relatively tight guarantee on the greedy decoder's performance.

Theorem V.2 (Greedy guarantee). Let G be a B-sensitive graph. Denote $\delta_* := \min_{v \in V} \deg(v)$ the minimum degree of G. Then the greedy graph decoder corrects at least $\lfloor \frac{\delta_*}{2B} \rfloor$ errors. In other words, the less sensitive a graph is, the more effective the greedy decoder. For constant B, the decoder thus corrects $\Theta(\delta_*)$ errors.

Proof. The decoder will fail if it makes either of the following two errors: (1) it applies $\texttt{Recover}_P(v)$ when v did *not* suffer a Pauli P error (Y errors are treated separately as both an X and a Z error) or (2) it fails to apply a $\texttt{Recover}_P(v)$ when v *did* suffer a Pauli P error. By the construction of the greedy decoder, this phenomenon occurs only if enough errors happened to flip at least $\lceil \frac{d}{2} \rceil$ lights in $o(v)$ or $oi(v)$, if v is a pivot. Indeed, in the former case, enough errors occurred to have turned on the majority of lights in $o(v)$ or $oi(v)$ without the corresponding error having occurred on v, and in the latter case it turned off the majority of lights even when the corresponding error occurred. Conditions (a)-(c) of Definition V.1 guarantee that it takes strictly more than $\lfloor \frac{1}{B} \lfloor \frac{\delta_*}{2} \rfloor \rfloor = \lfloor \frac{\delta_*}{2B} \rfloor$ errors to trick the decoder in either way during the X-recovery part of the algorithm, and condition (d) guarantees the same lower bound for the Z-on-pivots-recovery part of the algorithm. In condition (d), note that we equivalently used $o(u)$ for $u \in \mathcal{I}$ rather than $oi(u)$ for $u \in \mathcal{P}$ (as in the Z-on-pivots-recovery loop in Algorithm 1), and we have disregarded the $u = i(v)$ case which corresponds to an actual z error on $p(u)$ which would be correctly decoded. Thus, in all cases at least $\lfloor \frac{\delta_*}{2B} \rfloor$ errors are required to cause the decoder to act incorrectly, which completes the proof. $\square$

Recall that key code properties—weight of canonical stabilizers, distance, and canonical encoding circuit depth—are all bounded above by the degree. Because the number of errors corrected t and the distance are related by $2t + 1 \leq \text{dist}(C) \leq 2t + 2$, our result also implies a two-way bound on the distance of B-sensitive graphs.

Corollary V.2.1 (Distance bound)**.** Let G be a B-sensitive graph and minimum degree δ_*, and let $C(G)$ be the code that G represents. Then $\left\lfloor \frac{\delta_*}{B} \right\rfloor \leq 2\left\lfloor \frac{\delta_*}{2B} \right\rfloor + 1 \leq \mathrm{dist}(C(G)) \leq \delta_*$.

Similarly, we can give a bound on the encoding circuit based directly on the distance.

Corollary V.2.2 (Encoding circuit bound)**.** Let G be a B-sensitive graph and minimum degree δ_*. Let $C(G)$ be the code that G represents, and let $\mathcal{C}$ be its canonical encoding circuit as defined by the algorithm from Theorem IV.3. Then $\mathrm{depth}(\mathcal{C}) \leq \delta_* = 2B\frac{\delta_*}{2B} + B - B \leq B(2\left\lfloor \frac{\delta_*}{2B} \right\rfloor + 1) - B = B(\mathrm{dist}(C(G)) - 1)$.

The proof is an immediate consequence of Theorem IV.3 and Corollary V.2.1.

Although they are not necessary for the purposes of establishing Theorem V.2, several end-of-line optimizations to Algorithm 1 can improve its practical performance.

(1) *Neglecting destroyed lights.* Redefine `gap` to be the difference between the number of lights on in $o(v)$ and the number of lights that are *off but not destroyed* in $o(v)$. The only difference between this definition and the original is that lights which are destroyed are not counted. This follows because once a light is destroyed, it does not contribute to the QLO game anymore. Equivalently, a node with a destroyed light has already had some Pauli on it, which increased the weight of the total Pauli string by 1. Therefore, adding another Pauli to the same node does not increase the weight.

(2) *Gap edge case.* In the X loop, if `gap = 1` for the chosen node v, then only apply the recovery if the majority of un-destroyed lights in $oip(v)$ are on. This is because it costs one move in QLO to apply the recovery, and if the majority of lights are off in $oip(v)$ then one might actually turn more lights on than off by recovering, which could slightly increase the total number of moves.

(3) *Parity redundancy.* In the X recovery loop, consider only $o(v) \setminus oip(v)$ instead of $o(v)$, since lights in $o(v) \cap oip(v)$ cannot be turned on by X on v because $X(v)$ toggles each such light twice. Nodes in $o(v) \cap oip(v)$ can be affected by all other nodes which are neighbors of $p(v)$.

For a given graph code, a smaller sensitivity implies an increased effectiveness of the greedy decoder. We now give a family of codes for which the sensitivity is nearly optimal.

Previously, we defined in Section V A the hypercube code with parameters $[\![\frac{m2^m}{m+1}, \frac{2^m}{m+1}]\!]$. We label the nodes of the hypercube by their length-m binary string representation. Denote e_i the ith standard basis vector in $\mathbb{Z}_2^m$, i.e. $(e_i)_i = 1$ and $(e_i)_{j \neq i} = 0$. Moreover, we showed by injection of the classical Hamming code that the input nodes of the hypercube code are separated by paths of length at least 3. Before we prove that the hypercube has sensitivity 2, we give a useful lemma.

Lemma V.3 (Hypercube separation). It is possible to choose pivots on the hypercube code such that every path between pivots has length at least 3.

Proof. The minimum path length between inputs is already 3. By homogeneity of the hypercube, it is enough to choose the pivots in a uniformly consistent way for every input. One example which works is to set $p(v) = \{v + e_1\}$ for all $v \in \mathcal{I}$. This assignment will never choose $p(v) \in \mathcal{I}$ since the inputs are separated by paths of length at least 3. Now suppose there exists a path between two pivots p_1 and p_2 with length less than 3. In other words, with at most 2 bit flips, we can go from p_1 to p_2, so $p_2 = p_1 + e_a + e_b$ for some $a, b \in [m]$. Since $p_1 = i_1 + e_1$ and $p_2 = i_2 + e_1$, where i_j is the input corresponding to p_j, $i_2 = i_1 + e_a + e_b$, which contradicts the fact that inputs are separated by paths of length at least 3. $\square$

We note that there are several other transformations that can be applied to the hypercube to choose a set of pivots. One such other example is a $\frac{\pi}{2}$ axis-aligned rotation.

Theorem V.4 (Hypercube sensitivity). Every hypercube code is 2-sensitive.

Proof. By homogeneity, let $u = 0^m$ without loss of generality, so that $o(u)$ has only weight-1 bitstrings. We expand into each of the four cases in Definition V.1. The general idea is that when we take neighbour-type operations $p(\cdot), o(\cdot), i(\cdot)$ on a bitstring with weight M, the resultant bitstring's weight can only change by 1 due to the connectivity of the hypercube.

(a) Let $u, v \in \mathcal{O} \cup \mathcal{P}$. If $o(u) \cap (o(v) \Delta oip(v)) \neq \emptyset$, then $|v| \in \{2, 4\}$. These cases are shown in Fig. 9(1)-(2).

    i. If $|v| = 2$, let $v = e_i + e_j$ for $i \neq j$. So $o(u) \cap o(v) \subseteq \{e_i, e_j\}$. It is possible, as shown in Fig. 9(1) for $oip(v)$ to contain weight-1 bitstrings as well. Let's work forwards. By Lemma V.3, $p(v)$ has at most one element. Since inputs correspond
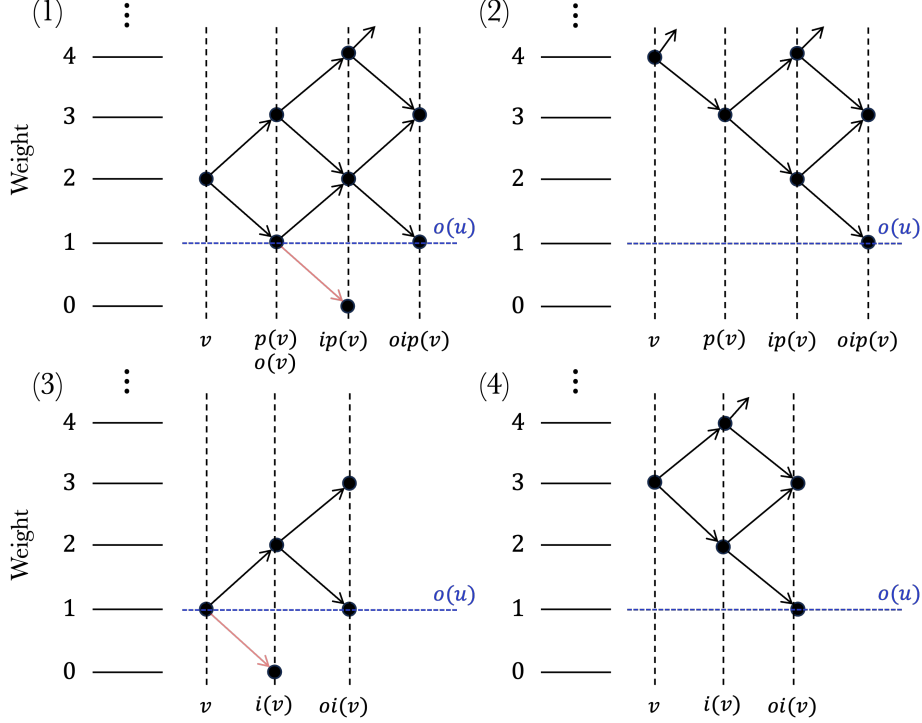
47

FIG. 9. Possible weights of nodes in a hypercube code after neighbouring operations (1) $o(v)$ and $oip(v)$ with starting weight $|v| = 2$, (2) $oip(v)$ with starting weight $|v| = 4$, (3) $oi(v)$ with starting weight $|v| = 1$, and (4) $oi(v)$ with starting weight $|v| = 3$. $u = 0^m$ in all cases, so $|w| = 1$ for all $w \in o(u)$. The red arrows correspond to paths that a priori seem possible but do not actually exist.

bijectively to pivots, $ip(v)$ thus also has at most one element. Suppose $\exists w \in ip(v)$. Then $oip(v)$ intersects $o(u)$ nontrivially only if $|w| \in \{0, 2\}$. However, u is the unique element whose weight is 0, and $u \notin \mathcal{I}$. Thus, since $w \in \mathcal{I}$, $|w| \neq 0$ so $|w| = 2$. Let $w = e_k + e_l$ for some $k \neq l$. Since w and v are separated by a path of length 2, $d_H(w, v) = 2$. Moreover, $|v| = 2$. The only way to transform $e_i + e_j \to e_k + e_l$ is if at least one of $\{e_i, e_j\}$ equals one of $\{e_k, e_l\}$. Without loss, say $e_i = e_k$. Then $o(u) \cap o(v) \subseteq \{e_i, e_j\}$ and $o(u) \cap oip(v) \subseteq \{e_i, e_l\}$, so $o(u) \cap (o(v) \triangle oip(v)) \subseteq \{e_j, e_l\}$, and hence $|o(u) \cap (o(v) \triangle oip(v))| \leq 2$.

ii. If $|v| = 4$, then $o(v)$ has weight at least 3, so the only possible intersection must come from $oip(v)$, as shown in Fig. 9(2). We argue similarly as before; namely that $ip(v)$ has at most one element, and if such an element w exists it must have weight 2 for $oip(v) \cap o(u) \neq \emptyset$. Write $w = e_i + e_j$ for $i \neq j$. Hence, $oip(v) = o(w)$

48

has at most two weight-1 elements, e_i and e_j. So $|o(u) \cap (o(v) \Delta oip(v))| \le 2$.

(b) In case (a) we showed that any nontrivial overlap with $o(v) \Delta oip(v)$ requires $|v| \equiv 0$ (mod 2). But $v \in o(u)$ only if $|v| = 1$. In the former case, i.e. $|v| \equiv 0$ (mod 2), $v \notin o(u)$, so we reduce to bounding $|o(u) \cap (o(v) \Delta oip(v))|$ which we have done already in case (a). In the latter case, $o(u) \cap (o(v) \Delta oip(v)) = \emptyset$ so $|o(u) \cap (\{v\} \Delta o(v) \Delta oip(v))| = |o(u) \cap \{v\}| \le 1$.

(c) Now $v \in \mathcal{P}$, and $u \in \mathcal{O} \cup \mathcal{P}$ as before. If $o(u) \cap oi(v) \ne \emptyset$, then $|v| \in \{1, 3\}$ as shown in Fig. 9(3)-(4). As seen earlier $|v| \equiv 0$ (mod 2) in order for $o(u) \cap (o(v) \Delta oip(v)) \ne \emptyset$. For $|v|$ even we have shown before the $B = 2$ bound. For $|v|$ odd it suffices to consider the overlap $o(u) \cap oi(v)$. Since $v \in \mathcal{P}$, $i(v)$ is the unique element w associated to the pivot v.

    i. If $|v| = 1$, then $|w| \in \{0, 2\}$ as shown in Fig. 9(3). Since $w \in \mathcal{I}$ and $u \notin \mathcal{I}$, $w \ne u$ so $|w| \ne 0$. Write $w = e_i + e_j$ for some $i \ne j$. Thus, $o(u) \cap oi(v) \subseteq \{e_i, e_j\}$, so $|o(u) \cap oi(v)| \le 2$.

    ii. If $|v| = 3$, then unless $|w| = 1$, $oi(v) \cap o(u) = \emptyset$ as shown in Fig. 9(4). Then $w = e_i + e_j$ for $i \ne j$, so $o(u) \cap oi(v) \subseteq \{e_i, e_j\}$ and thus $|o(u) \cap oi(v)| \le 2$.

(d) Now, $u \in \mathcal{I}$, $v \in \mathcal{P}$, and $u \ne i(v)$. This case has essentially already been proven by part (c). The only difference is that the input node $w = i(v)$ cannot have weight 0 because $u \ne i(v)$.

$\square$

As a consequence of the optimal sensitivity of the hypercube, we can not only correct its errors well by a greedy approach, but also obtain a good distance lower bound that is at most a factor of 2 from optimal.

Corollary V.4.1. The d-dimensional hypercube cube has distance between $2 \lceil \frac{d}{4} \rceil + 1 \approx d/2$ and d.

We believe that a more careful analysis requiring detailed casework can show that our algorithm is correct up to $\frac{d}{2}$ errors, and thus distance d. However, this example already shows

that we can use this formalism to construct graphs that give simple and intuitive algorithms for decoding.

Conjecture V.5. The d-dimensional hypercube code has distance d and a greedy decoding algorithm can decode up to $\lfloor \frac{d-1}{2} \rfloor$ errors.

C. Random codes with reduced stabilizer weights

One direct technique for which a graph formalism enables more controlled analysis is random codes. Under the stabilizer tableau representation, the quantum Gilbert-Varshamov-bound gives an asymptotic (large n) relation between code parameters n, k, d that, if satisfied, guarantee the existence of a $[\![n, k, d]\!]$ code.

Theorem V.6 (Quantum Gilbert-Varshamov)**.** For parameters $d \leq \frac{n}{2}$, k which depend implicitly on n, as $n \to \infty$ there exists a $[\![n, k, d]\!]$ code if $nH(d/n) + d \log 3 < n - k$, where $H(p) := -p \log p - (1 - p) \log(1 - p)$ is the binary entropy function of $p \in [0, 1]$.

We give a self-contained proof of Theorem V.6 in Appendix C. The proof proceeds probabilistically, namely by generating a uniformly random stabilizer tableau and arguing that such a tableau has a nonzero probability of having distance d if the bound is satisfied. However, because the expected weight (i.e. number of non-identity elements) of a random Pauli string $P_1 \otimes \cdots \otimes P_n$, where $P_i \in \{I, X, Y, Z\}$, is $O(n)$, the random codes generated in the Gilbert-Varshamov fashion will have linear stabilizer weight. A natural question is whether the average weight can be decreased by a stochastic algorithm that is more fine-grained than uniform randomness. Such a task has proven difficult in the stabilizer tableau representation due to the challenge of generating Paulis that both commute and are not uniformly distributed. On the other hand, we can easily generate random graphs of a certain structure by defining first the possible edges that may be included, and then randomly choosing edges to include in the graph. This insight enables us to extend the result of the quantum Gilbert-Varshamov bound by way of the following theorem.

Theorem V.7. Let n be the number of physical qubits and define $R(n) < 1$ and $d(n) \in [\omega(1), \frac{n}{\log n}]$. There exists an efficiently sampleable family of distributions $\mathcal{S}_n$, parameterized by n, over stabilizer codes that as $n \to \infty$ satisfy three properties.

(a) The stabilizer weights are

$$|S_i| \leq \min(n, (4 + o(1))Rd^2 \log^2 n), \tag{15}$$

where S_i is a stabilizer from a tableau sampled from $\mathcal{S}_n$,

(b) the rate is $R(n)$, and

(c) with probability at least $1 - n^{-d}$, a random code from $\mathcal{S}_n$ will have distance $d(n)$.

We remark that the idea of finding a smaller class of objects which achieve desirable properties is conceptually similar to an idea explored recently by Cleve *et al.* [64], who showed that there is a strict subgroup of the Clifford group that also uniformly mixes non-identity Paulis.

Theorem V.7 is positive in that it provides a nontrivial bound on the stabilizer weight of random codes for many choices of $R(n)$ and $d(n)$, and it gives a strong probabilistic concentration of a $1 - n^{-d}$. For any $d \in [\omega(1), O(\frac{n}{\log n})]$, this concentration implies that almost all codes in $\mathcal{S}_n$ have the desired properties. On the other hand, Theorem V.7 complements—as opposed to subsuming—the Gilbert-Varshamov bound because it provides a nontrivial weight reduction at substantially sublinear distances. It also forces the stabilizer weight—at least, for the generating set we construct—to be at least as large as the distance, which is an artifact of our proof technique. However, the result nonetheless remains interesting because of the guarantees it is able to provide and the flexibility that it offers. Indeed, practically useful codes are seldom asymptotically good. Since the distance and the rate are both determining factors for the stabilizer weight, we obtain a three-way distance-rate-weight tradeoff of random codes that can be leveraged to study sublinear-distance codes in which we care much less about one of the three properties than the others. As with the other claims in this paper, this result is thus complementary of LDPC constructions that are asymptotically good but have intractably large constants. Instead, we interpret this result as evidence that for moderately large codes—e.g. $n \sim 50$ at a scale where we expect little-o asymptotics to take effect—there is a great deal of flexibility in the graph construction to build codes of certain ranges of R and d which also may have a relatively small stabilizer weight.
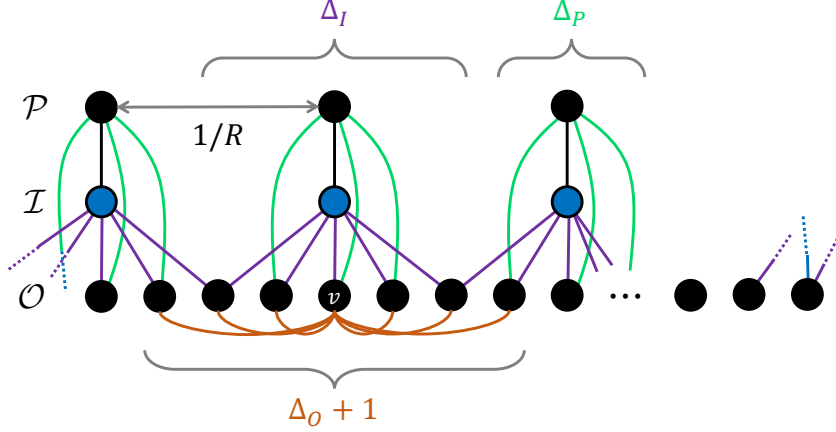
We proceed to the proof of Theorem V.7.

FIG. 10. General localized random graph construction. Nodes are separated into k input nodes $i \in \mathcal{I}$, (which are spaced apart by $1/R$), k pivot nodes $p \in \mathcal{P}$, and $n - k$ non-pivot output nodes $o \in \mathcal{O}$. Each pivot p (input i) can connect to output nodes within a diameter Δ_P of p (Δ_I of i); here, $\Delta_P = 3$ ($\Delta_I = 5$) and the possible lines are green (purple). Similarly, output nodes o may connect to outputs in a diameter Δ_O of o. For clarity, only the possible connections for a single output v is shown, and here $\Delta_O = 6$.

Proof. We construct elements of $\mathcal{S}_n$ graphically as shown in Fig. 10; denote this graph G. In particular, we begin with an encoder-respecting form, separating the inputs $\mathcal{I}$, pivots $\mathcal{P}$, and (non-pivot) outputs $\mathcal{O}$. Next, we assign each set of nodes a *locality diameter*, respectively $\Delta_I, \Delta_P, \Delta_O + 1$ (the $+1$ since the output node is included in its diameter but does not have a self-edge). The boundary conditions are periodic. Each node may only connect to output nodes within their locality diameter. We sample from $\mathcal{S}_n$ by iterating through each connectable edge and randomly including or excluding it from the graph with probability $1/2$; the resulting stabilizer tableau is the one defined by the collection $S := \{S_v := X(v)Z(N_o(v))X(p(i(v)))Z(N_o(p(i(v))))\}_{v \in \mathcal{O}}$ as described in Section IV. For notation, we say that S_v contains a Pauli X_i (Z_i) if the ith element of S_v is X_i or Y_i (Z_i or Y_i). Our analysis of this stochastic algorithm adapts the techniques in the analysis of Theorem V.6 to the graph picture. We fix a non-identity Pauli P and consider four cases.

(1) $P = Z^{\otimes T}$ for $T \subseteq [n]$ and T does not contain any pivots. Pick $i \in T$ and consider $v_i \in G$. Then S_{v_i} must anticommute with P because S_{v_i} contains $X(v_i)X(p(i(v_i)))$ which only overlaps P in one position. Hence, P does not commute with S.

(2) $P = Z^{\otimes T}$ for $T \subseteq [n]$ and T contains at least one pivot $p \in \mathcal{P}$. Let $i \in \mathcal{I}$ be the unique input connected to p. Each of the Δ_I output nodes v within the diameter Δ_I of i have probability $1/2$ of connecting to i. S_v contains $X(p)$ if and only if i and v are connected. Since the (anti-)commutativity of P and S_v are determined only by the parity of the number of qubits on which X's in S_v overlap with Z's in P, the probability that S_v and P commute is $1/2$ regardless of the other Paulis in S_v and P. Furthermore, consider any other S_w where w is also in the diameter of i. Because w has an edge connecting to i distinct from that of v, the probability of S_w and P commuting is independently $1/2$. This argument is general to all output nodes in the diameter of i, and remaining stabilizer act on disjoint subspaces. Hence the probability that P commutes with S is $2^{-\Delta_I}$.

(3) P contains at least one $X(p)$ for $p \in \mathcal{P}$. Analogously, $\Pr[P \text{ commutes with } S] = 2^{-\Delta_P}$ by considering the Δ_P nodes in $\mathcal{O}$ which each independently have probability $1/2$ of having a $Z(p)$.

(4) P contains at least one $X(v)$ for $v \in \mathcal{O}$. $\Pr[P \text{ commutes with } S] \leq 2^{-\Delta_O}$ by an analogous argument. We neglect some stabilizers which could anticommute with P by acting through neighbouring pivots, i.e. the $Z(N_o(p(i(v))))$ component, since that can only decrease the probability and complicates the expression.

Set $\Delta_O = \Delta_P = \Delta_I := \Delta$. We proceed to bound the probability of the event $A(S)$ that there exists non-identity P with weight $\leq d$ which commutes with S. As shown in Appendix C, there are $2^{nH(d/n)+d\log 3+O(\log n)}$ such Paulis, where $H(p) = -p\log p - (1-p)\log(1-p)$ is the binary entropy. By the union bound,

$$\Pr[A(S)] \leq 2^{nH(d/n)+d\log 3+O(\log n)-\Delta} \leq \epsilon, \tag{16}$$

where ϵ bounds the fraction of codes which do not have distance at least d. We therefore solve the equation

$$\Delta \geq \log\frac{1}{\epsilon} + nH\left(\frac{d}{n}\right) + d\log 3 + O(\log n). \tag{17}$$

Since $\frac{d}{n} \leq \frac{1}{\log n}$, we can asymptotically expand the binary entropy as $H(d/n) \to (\frac{1}{\ln 2} - \log\frac{d}{n})\frac{d}{n}$,

53

giving

$$\Delta \geq \log \frac{1}{\epsilon} + d \log n + o(d \log n). \tag{18}$$

Here we have used our assumption that $d = \omega(1)$, so that $O(\log n) = o(d \log n)$. Let $\epsilon = n^{-d}$, so that if $\Delta = 2d \log n + o(d \log n)$ at least $1 - n^{-d}$ of codes asymptotically have distance d. Lastly, we calculate the stabilizer weights. Each stabilizer is of the form $S_v = X(v)Z(N_o(v))X(p(i(v)))Z(N_o(p(i(v))))$. These terms have at most 1, Δ_O, $\Delta_I R$, and $\Delta_P(\Delta_I R)$ Paulis, assuming no overlap and all edges are connected. Hence,

$$|S_v| \leq 1 + \Delta + \Delta R + \Delta^2 R = (4 + o(1))Rd^2 \log^2 n. \tag{19}$$

Obviously, $|S_v| \leq n$, which gives the claimed result. $\qquad\square$

An important special case of Theorem V.7 is for graphs in which all inputs are at least 3 nodes away from each other, in which case $R = 1/\Delta$ and thus $|S_v| \leq (2 + o(1))d \log n$.

VI. CONCLUSION & OUTLOOK

We introduced a graph structure which universally represents all stabilizer codes. Stabilizer tableaus can be efficiently compiled into such graphs, and vice versa. Our primary motivation for such a representation was to gain access to natural graph properties and notions—degree, geometry, connectivity—and then leverage them to improve code construction and analysis. As first steps in this direction, we chose several geometric shapes discretized into graphs and analyzed them as code representations. In doing so, we found a number of constant-size codes with desirable rates and reasonably large numerical distances, as well as a family of hypercube codes that have near-linear rate, logarithmic distance, and good encoding/decoding properties. In similar spirit, we also constructed a class of codes for which, given a desired rate R and distance d, a random code drawn from the class has high probability of having rate R, distance d, and, so long as R and d were not both too large, nontrivially bounded stabilizer weights. This analysis extends the result of the quantum Gilbert-Varshamov bound, which has a distance-rate tradeoff but no bound on stabilizer weight due to its coarse-grained analysis.

More generally, we showed that graph properties are intimately tied to code properties. Key code properties (weight, distance, encoding and logical operator circuit depths) are all

controlled by small linear functions of graph degrees, and key coding algorithms (distance approximation, weight reduction, decoding) are all strategies on various instances of quantum lights out (QLO) games. The former observation allowed us to leverage graph algorithms to efficiently construct encoding circuits with controlled depth upper bounds as well as build logical operation circuits whose depths, in the case of diagonal or certain Clifford gates, are conceptually distinct and quantitatively better than simply unencoding, applying, and re-encoding. The latter result led us to design an efficient greedy QLO strategy for decoding, and prove that it succeeds up to a small constant factor on at least a certain class of graphs which include the hypercube code. We believe that further study in graph-based decoding algorithms will reveal efficient decoders for many other families of graphs. In sum, the universal graph representation enables insights and improvements that are general across all or large classes of stabilizer codes, by providing avenues of construction and analysis that are substantially less obvious via conventional representations of additive quantum codes.

There are several directions in which to explore from this point. The first is general. Classically, graph representations have shown a strong correspondence between graph properties and code properties beyond simple objects like the degree. Notably, spectral expander graphs have led to good classical codes. A characterization effort connecting graph properties such as spectrum, expansion, cycle sizes, density, geometry, and topology to distance, decoding, stabilizer weight, etc. could significantly extend this work's insight into stabilizer codes. It is also worthwhile to more deeply study the quantum lights out game, as insights onto their strategies have equivalent interpretations on coding algorithm performance. First steps towards the worst- and average-case analysis of coding algorithms based on the hardness of certain computational problems have appeared recently [65], and their connection to QLO is an interesting question. A second direction is directly constructive. Given particular architectures or algorithms of experimental interest, is it possible to systematically design graphs whose codes are particularly suitable for such devices or algorithms in terms of locality of connectivity, geometry, rate, and distance? The third involves refining the approach of this work. Representations that are universal are doomed in certain aspects of coding because their generality implies that properties scale with distance. If there exists a collection of graphs that, in exchange for representing a restricted subset of stabilizer codes, satisfies low-weight stabilizers, it may open new paths forward for practical code constructions and

corresponding algorithms. Such a representation would essentially lie in an optimal middle ground between the approach of surface-type code constructions and the universal graph representation.

[1] L. K. Grover, A fast quantum mechanical algorithm for database search, in *Proceedings of the twenty-eighth annual ACM symposium on Theory of computing* (1996) pp. 212–219.

[2] P. W. Shor, Polynomial-time algorithms for prime factorization and discrete logarithms on a quantum computer, SIAM review **41**, 303 (1999).

[3] Z. Brakerski, P. Christiano, U. Mahadev, U. Vazirani, and T. Vidick, A cryptographic test of quantumness and certifiable randomness from a single quantum device, Journal of the ACM (JACM) **68**, 1 (2021).

[4] E. Farhi, D. Gosset, A. Hassidim, A. Lutomirski, and P. Shor, Quantum money from knots, in *Proceedings of the 3rd Innovations in Theoretical Computer Science Conference* (2012) pp. 276–289.

[5] I. M. Georgescu, S. Ashhab, and F. Nori, Quantum simulation, Reviews of Modern Physics **86**, 153 (2014).

[6] H.-Y. Huang, R. Kueng, and J. Preskill, Predicting many properties of a quantum system from very few measurements, Nature Physics **16**, 1050 (2020).

[7] A. Harrow, P. Hayden, and D. Leung, Superdense coding of quantum states, Physical review letters **92**, 187901 (2004).

[8] M. A. Nielsen and I. Chuang, Quantum computation and quantum information (2002).

[9] A. Kandala, K. Temme, A. D. Córcoles, A. Mezzacapo, J. M. Chow, and J. M. Gambetta, Error mitigation extends the computational reach of a noisy quantum processor, Nature **567**, 491 (2019).

[10] M. V. Larsen, X. Guo, C. R. Breum, J. S. Neergaard-Nielsen, and U. L. Andersen, Deterministic generation of a two-dimensional cluster state, Science **366**, 369 (2019).

[11] F. Arute, K. Arya, R. Babbush, D. Bacon, J. C. Bardin, R. Barends, R. Biswas, S. Boixo, F. G. Brandao, D. A. Buell, *et al.*, Quantum supremacy using a programmable superconducting processor, Nature **574**, 505 (2019).

[12] H. Wang, J. Qin, X. Ding, M.-C. Chen, S. Chen, X. You, Y.-M. He, X. Jiang, L. You, Z. Wang, *et al.*, Boson sampling with 20 input photons and a 60-mode interferometer in a 1 0 14-dimensional hilbert space, Physical review letters **123**, 250503 (2019).

[13] C. K. Andersen, A. Remm, S. Lazar, S. Krinner, N. Lacroix, G. J. Norris, M. Gabureac, C. Eichler, and A. Wallraff, Repeated quantum error detection in a surface code, Nature Physics **16**, 875 (2020).

[14] A. Y. Kitaev, Quantum error correction with imperfect gates, in Quantum communication, computing, and measurement (Springer, 1997) pp. 181–188.

[15] S. B. Bravyi and A. Y. Kitaev, Quantum codes on a lattice with boundary, arXiv preprint quant-ph/9811052 10.48550/arXiv.quant-ph/9811052 (1998).

[16] A. G. Fowler, M. Mariantoni, J. M. Martinis, and A. N. Cleland, Surface codes: Towards practical large-scale quantum computation, Physical Review A **86**, 032324 (2012).

[17] P. W. Shor, Scheme for reducing decoherence in quantum computer memory, Physical review A **52**, R2493 (1995).

[18] D. Gottesman, An introduction to quantum error correction and fault-tolerant quantum computation, arXiv preprint arXiv:0904.2557 10.48550/arXiv.0904.2557 (2009).

[19] D. Gottesman, Stabilizer codes and quantum error correction (California Institute of Technology, 1997).

[20] A. Steane, Multiple-particle interference and quantum error correction, Proceedings of the

Royal Society of London. Series A: Mathematical, Physical and Engineering Sciences **452**, 2551 (1996).

[21] A. R. Calderbank and P. W. Shor, Good quantum error-correcting codes exist, Physical Review A **54**, 1098 (1996).

[22] S. Aaronson and D. Gottesman, Improved simulation of stabilizer circuits, Physical Review A **70**, 052328 (2004).

[23] J.-P. Tillich and G. Zémor, Quantum ldpc codes with positive rate and minimum distance proportional to the square root of the blocklength, IEEE Transactions on Information Theory **60**, 1193 (2013).

[24] N. P. Breuckmann and J. N. Eberhardt, Balanced product quantum codes, IEEE Transactions on Information Theory **67**, 6653 (2021).

[25] P. Panteleev and G. Kalachev, Degenerate quantum ldpc codes with good finite length performance, Quantum **5**, 585 (2021).

[26] M. Sipser and D. A. Spielman, Expander codes, IEEE transactions on Information Theory **42**, 1710 (1996).

[27] A. Y. Kitaev, Fault-tolerant quantum computation by anyons, Annals of physics **303**, 2 (2003).

[28] S. Bravyi, A. W. Cross, J. M. Gambetta, D. Maslov, P. Rall, and T. J. Yoder, High-threshold and low-overhead fault-tolerant quantum memory, Nature **627**, 778 (2024).

[29] J. Edmonds, Maximum matching and a polyhedron with 0, 1-vertices, Journal of research of the National Bureau of Standards B **69**, 55 (1965).

[30] J. Edmonds, Paths, trees, and flowers, Canadian Journal of mathematics **17**, 449 (1965).

[31] T. Bergamaschi, L. Golowich, and S. Gunn, Approaching the quantum singleton bound with approximate error correction, in *Proceedings of the 56th Annual ACM Symposium on Theory of Computing* (2024) pp. 1507–1516.

[32] T. Rakovszky and V. Khemani, The physics of (good) ldpc codes ii. product constructions, arXiv preprint arXiv:2402.16831 (2024).

[33] A. Ashikhmin, S. Litsyn, and M. A. Tsfasman, Asymptotically good quantum codes, Physical Review A **63**, 032311 (2001).

[34] P. Panteleev and G. Kalachev, Asymptotically good quantum and locally testable classical ldpc codes, in *Proceedings of the 54th Annual ACM SIGACT Symposium on Theory of Computing*

(2022) pp. 375–388.

[35] A. T. Hu and A. B. Khesin, Improved graph formalism for quantum circuit simulation, Physical Review A **105**, 022432 (2022).

[36] T. McElvanney and M. Backens, Complete flow-preserving rewrite rules for mbqc patterns with pauli measurements, arXiv preprint arXiv:2205.02009 10.4204/EPTCS.394.5 (2022).

[37] S. Yu, Q. Chen, and C. H. Oh, Graphical quantum error-correcting codes, arXiv preprint arXiv:0709.1780 (2007).

[38] A. Kissinger, Phase-free zx diagrams are css codes (... or how to graphically grok the surface code), arXiv preprint arXiv:2204.14038 10.48550/arXiv.2204.14038 (2022).

[39] Z. Wu, S. Cheng, and B. Zeng, A zx-calculus approach to concatenated graph codes, arXiv preprint arXiv:2304.08363 10.48550/arXiv.2304.08363 (2023).

[40] N. Chancellor, A. Kissinger, S. Zohren, J. Roffe, and D. Horsman, Graphical structures for design and verification of quantum error correction, Quantum Science and Technology 10.1088/2058-9565/acf157 (2016).

[41] A. B. Khesin and A. Li, Equivalence classes of quantum error-correcting codes, arXiv preprint arXiv:2406.12083 (2024).

[42] B. Coecke and R. Duncan, Interacting quantum observables, in *International Colloquium on Automata, Languages, and Programming* (Springer, 2008) pp. 298–310.

[43] T. Peham, L. Burgholzer, and R. Wille, Equivalence checking of quantum circuits with the zx-calculus, IEEE Journal on Emerging and Selected Topics in Circuits and Systems **12**, 662 (2022).

[44] A. Cowtan and S. Majid, Quantum double aspects of surface code models, Journal of Mathematical Physics **63**, 042202 (2022).

[45] J. van de Wetering, Constructing quantum circuits with global gates, New Journal of Physics **23**, 043015 (2021).

[46] R. D. East, J. van de Wetering, N. Chancellor, and A. G. Grushin, Aklt-states as zx-diagrams: diagrammatic reasoning for quantum states, PRX Quantum **3**, 010302 (2022).

[47] N. de Beaudrap and D. Horsman, The zx calculus is a language for surface code lattice surgery, Quantum **4**, 218 (2020).

[48] A. Kissinger and J. van de Wetering, Reducing the number of non-clifford gates in quantum

circuits, Physical Review A **102**, 022406 (2020).

[49] M. Backens, The zx-calculus is complete for stabilizer quantum mechanics, New Journal of Physics **16**, 093021 (2014).

[50] R. Duncan, A. Kissinger, S. Perdrix, and J. Van De Wetering, Graph-theoretic simplification of quantum circuits with the zx-calculus, Quantum **4**, 279 (2020).

[51] J. van de Wetering, Zx-calculus for the working quantum computer scientist, arXiv preprint arXiv:2012.13966 10.48550/arXiv.2012.13966 (2020).

[52] R. Duncan and M. Lucas, Verifying the steane code with quantomatic, arXiv preprint arXiv:1306.4532 10.48550/arXiv.1306.4532 (2013).

[53] E. Knill, R. Laflamme, R. Martinez, and C. Negrevergne, Benchmarking quantum computers: The five-qubit error correcting code, Physical Review Letters **86**, 5811 (2001).

[54] A related discussion of such a transformation is given in a simultaneous work by one of the authors in Khesin and Li [41].

[55] V. G. Vizing, On an estimate of the chromatic class of a p-graph, Diskret. Analiz. **3**, 25 (1964).

[56] J. Misra and D. Gries, A constructive proof of vizing's theorem, Information Processing Letters **41**, 131 (1992).

[57] We adopt the name quantum lights out because the game appears to be a generalization of a classical game known as lights out, in which a player aims to turn all lights off on a grid with some lights initially on, using moves such that flipping a switch at a given cell toggles all adjacent cell's lights but not their own. QLO generalizes this notion onto a general graph, and adds more flexibility on how lights may be toggled.

[58] U. Kapshikar and S. Kundu, On the hardness of the minimum distance problem of quantum codes, IEEE Transactions on Information Theory **69**, 6293 (2023).

[59] R. Tanner, A recursive approach to low complexity codes, IEEE Transactions on information theory **27**, 533 (1981).

[60] J. Z. Lu and A. B. Khesin, graphcodes.

[61] A. Couvreur, N. Delfosse, and G. Zémor, A construction of quantum ldpc codes from cayley graphs, IEEE transactions on information theory **59**, 6087 (2013).

[62] F. Pastawski, B. Yoshida, D. Harlow, and J. Preskill, Holographic quantum error-correcting codes: Toy models for the bulk/boundary correspondence, Journal of High Energy Physics

2015, 1 (2015).

[63] R. W. Hamming, Error detecting and error correcting codes, The Bell system technical journal **29**, 147 (1950).

[64] R. Cleve, D. Leung, L. Liu, and C. Wang, Near-linear constructions of exact unitary 2-designs, arXiv preprint arXiv:1501.04592 (2015).

[65] A. Poremba, Y. Quek, and P. Shor, The learning stabilizers with noise problem, arXiv preprint arXiv:2410.18953 (2024).

Appendix A: Tableau to Graph Proofs

In the main text, we sketched briefly the algorithm that maps encoders to ZXCFs. Here, we give a detailed explication. The first part of our algorithm maps the encoder into *some* ZX diagram; we can then transform it via a sequence of equiavlence rules into a ZXCF. To accomplish a transformation into ZX diagrams, we first observe prior work by Hu and Khesin [35] for stabilizer states.

Theorem A.1 (Hu and Khesin [35]). There exists a ZXCF for stabilizer quantum states, which we call the HK form.

Although Hu and Khesin did not use ZX calculus in their work, their construction uses graph states decorated with single-qubit operators, which can be mapped directly to ZX calculus by a manner we will briefly describe. A HK diagram is constructed by starting with a graph state—a state corresponding to an undirected graph wherein the nodes become $|+\rangle$ qubits and the edges become controlled-Z gates. Each node is then endowed with a single *free edge*, which does not connect to any other node. Local Clifford operations in $\langle H, S, Z \rangle$ are then applied to the qubits. Such a construction has the capacity to express any stabilizer state. A direct mapping enables the presentation of a HK diagram into the ZX calculus.

(1) HK vertices become Z nodes, as a vertex in a graph state begins in the state $|+\rangle$, which is a Z node with a single output.

(2) HK (non-free) edges become (non-free) edges with Hadamard gates, as both of these correspond to CZ gates.

(3) HK local operations of S, Z, or SZ become phases on the corresponding node of $\frac{\pi}{2}$, π, and $\frac{3\pi}{2}$, respectively. The local operation H becomes a Hadamard gate on the node's free edge.

Thus, we will without loss consider HK forms to be in the ZX calculus representation and denote them *ZX-HK forms*. We remark that transformations of similar decorated graph state families into ZX calculus presentations have been considered in other contexts, such as in Backens [49].

The work of Hu and Khesin [35] is limited to stabilizer states. However, by vector space duality one can equivalently transform operators into states and vice versa. (The formal statement of this duality in quantum information theory is given by the Choi-Jamiołkowski isomorphism.) The composition of such a transformation with the result above gives the following lemma.

Lemma A.2. There exists an efficient transformation of a ZX encoder diagram with $n - k$ input edges and n output edges into a corresponding ZX presentation of a stabilizer state in ZX-HK form, with $n + (n - k) = 2n - k$ free edges.

Proof. We will turn the encoder diagram into a Clifford circuit, and then map the output of that circuit (with input the all-$|+\rangle$ state) to HK form. Any X (red) nodes in the ZX encoder diagram can be transformed into Z (green) nodes with the same phase surrounded by Hadamard gates. Now, we can interpret the ZX encoder diagram as a state by treating the input edges as output edges (the ZX version of the Choi-Jamiołkowski isomorphism).

Our ZX diagram now computes a state, so we can express it entirely in terms of the following elementary operations and their circuit analogs. First, we could have a Z node with only one output or only one input. In a circuit, this is a $|+\rangle$ qubit or a post-selected $\langle +|$ measurement, respectively. We can also have a Hadamarded edge or a node with $\frac{\pi}{2}$ phase, which are represented as H or S gates in circuits, respectively. Lastly, we can have a Z node of degree 3, with either 2 inputs and 1 output or 1 input and 2 outputs that acts as a merge or a split. This is equivalent to applying a CX operation between two qubits where the second qubit is either initialized to $|0\rangle$ before the CX gate or post-selected by the measurement $\langle 0|$ after the CX gate, respectively.

Any ZX diagram can be expressed in terms of these operations [49]. Furthermore, as we apply each of these operations we can keep track of the current HK form for our state. (The Hu and Khesin [35] method shows us how to keep a diagram in HK form as each operation is applied.) All of these steps can be done efficiently [35], so this gives us an efficient procedure for turning a ZX diagram into a corresponding stabilizer state in HK form. □

Application of Lemma A.2 results in a ZX-HK form. That is, there is one Z node per vertex of the graph in HK form, with any internal edge having a Hadamard gate on it. Free edges can only have Hadamard gates on them if their phase is a multiple of π, corresponding

to the local Clifford gates H and HZ in HK form, and if the associated node is not connected to any lower-numbered nodes. Nodes whose free edges have no Hadamard gate are free to have any multiple of $\frac{\pi}{2}$ as a phase, corresponding to local Clifford operations I, S, Z, or SZ, respectively.

We are now equipped with a ZX-HK diagram that represents a state. This diagram has only output edges. To return it into an encoder diagram, we partition the $2n - k$ free edges into $n - k$ input edges and n output edges. In the circuit representation, this is equivalent to turning bra's into ket's and vice versa to map between an operator and a state. For example, $|00\rangle \langle 1| - |11\rangle \langle 0| \leftrightarrow |001\rangle - |110\rangle$. Now, if there are any edges between input nodes (those in $\mathcal{I}$), we can simply remove them. They correspond to controlled-Z operations, and we can take off any unitary operation on the input by the encoder definition. The same goes for local Cliffords on $\mathcal{I}$.

At this stage, the obtained ZX-HK form is in encoder-respecting form. It also satisfies the Edge and Hadamard rules—there are no input edges in ZX-HK form so the analogous rule is enforced only on lowered-numbered nodes, but if we number the nodes from the beginning such that the input nodes are lowered-numbered than all output nodes, then the transformed ZX-HK form will satisfy our ZXCF Hadamard rule. So, all that remains is to simplify the diagram to obey the RREF and Clifford rules.

Lemma A.3. An encoder diagram in ZX-HK form can be efficiently transformed to satisfy the RREF rule, while continuing to satisfy the Edge and Hadamard rules.

Proof. This proof relies on two basic properties of ZX calculus. The first is that a CX gate can be expressed on a pair of qubits by applying a pair of spiders connected by an edge, with a Z spider on the control and an X spider on the target. The second fact is a rewrite rule called the *bialgebra rule* [49], which allows us to rewrite a green node connected to a red node by the following sequence of steps. First, remove the two spiders and the edge between them. Next, add a red node on each edge previously leading into the green node; do the same for the red node by adding green nodes. Lastly, connect each red node to each green node.

Applying a CX gate to a pair of inputs is a unitary operation and does not change our code. The control spider of the CX gate fuses with the first input. The target spider is used to perform the bialgebra rule with the second input. This results in two green nodes where

the CX target used to be. The first is merged with the first input while the second takes the place of the recently-destroyed second input. Meanwhile, the red nodes on each input-output edge previously connected to the second input now find themselves connected to both the first and second input, and turn green after commuting through the Hadamard gate on the input-output edge, merging with the output on the other side. Any doubled edges are removed by the Hopf rule [49]. The result is that we added the row of $M_\mathcal{D}$ corresponding to the first input the the row of the second. This allows to do arbitrary row operations since we are working in a field of characteristic 2. This concludes the proof of the fact that $M_\mathcal{D}$ can be turned into RREF without affecting the Edge and Hadamard rules.

$\square$

The only remaining task is to enforce the Clifford rule. For any pivot node $p \in \mathcal{P}$ with a non-zero phase, denote v_in its associated input node. We apply a local complementation about v_in, which notably does not change the entries of $M_\mathcal{D}$. However, this operation also increases the phase of each neighbours of v_in by $\frac{\pi}{2}$ (due to multiplication by S) so we repeat this process until the phase of that pivot vanishes. The local complementation transformation is a ZX equivalence identity, and therefore is a valid operation on our diagram [49].

Lastly, if there are any edges between pivots p_1 and p_2, we can remove them by applying a different transformation ϕ to their pair of associated input nodes v_1 and v_2. Let N_1 be the set of the neighbours of v_1 as well as v_1 itself and let N_2 be defined respectively. The effect of ϕ is to toggle all edges in the set $N_1 \times N_2$, including multiplicity. This means that edges that get toggled twice are not affected. Any self-edge of the form (v, v) is treated as a Z operation on vertex v. In addition, ϕ also applies an additional local operation of HZ to each of v_1 and v_2, but this can be removed as v_1 and v_2 are input vertices. As a result of this, we have swapped the neighbours of v_1 and v_2 as well as toggled the one pivot-pivot edge we wish to flip, (p_1, p_2). Note that ϕ does not violate the RREF rule because once this process is complete we can simply swap the neighbours back (without any toggling) via a row operation. This also does not add any local operations to the nodes p_1 and p_2, as each is only in one of N_1 and N_2, and thus does not receive a Z operation. We repeat until no pivot-pivot edges remain. ϕ can be shown to be a valid ZX equivalence identity from Eqn. (101) in van de Wetering [51].

With that step, the transformation from Clifford encoder to ZXCF is complete. Although

this process may seem lengthy, all of these steps can be done systematically in an efficient manner, without having to go back to fix earlier rules. Specifically, this algorithm takes $O(n^3)$ time. Creating the HK diagram for the encoder requires us to apply $O(n)$ Pauli projections, each of which can be applied in $O(n^2)$ time. After the HK form is created, operations such as row-reducing a matrix also take $O(n^3)$ time. We suspect that the time complexity cannot be improved in the worst case, but that there is a lot of room for heuristic runtime improvements and optimizations.

Appendix B: Derivation of the ZXCF counting recursion

We conclude this section with the derivation of the recursive counting formula of ZXCF diagrams, given in Eq. (3). To derive f, imagine that, starting with two empty bins, we must assign the $n - k$ output nodes to be pivots (case A) or non-pivots (case B), where pivots need to be matched with input nodes. The current number of pivots is tracked by p and the number of non-pivot outputs is tracked by o.

Suppose we want the next output node to be a pivot (in $\mathcal{P}$). Since there is a one-to-one correspondence between pivots and inputs, we can add pivots only if $n > k$. The matching between pivots and input nodes is fully constrained by the RREF rule, which sorts the inputs and pivots together. The Clifford rule says that no pivot nodes may have local Clifford operations, so we just need to choose the edges connecting them to nodes we have already assigned. Since there are no pivot-pivot edges and the pivot connects to only one input, we have exactly 2° possibilities. Having made an assignment, p increases by 1, and n decreases by 1 (both input and output are decremented since the pivot matches with an input).

Suppose instead we want the next output node to be a non-pivot (in $\mathcal{O}$). Then we have to choose the local Clifford operation as well as its edges to previously assigned vertices. If we choose to connect the node to none of the p assigned inputs, p assigned pivots, or o assigned vertices, then we are allowed to place any of the 6 local Cliffords on the node. If any of those edges are present, however, we cannot apply a Hadamard to the output edge due to the Hadamard rule. Hence, 4 choices remain for the local Clifford operation. This works out to a total of $4(2^{2p+o} - 1) + 6 = 2^{2p+o+2} + 2$ possibilities. To finish, we decrement

66

the number of output qubits without changing the number of inputs.

Appendix C: Quantum Gilbert-Varshamov

The quantum Gilbert-Varshamov bound, Theorem V.6, is discussed in, e.g., Nielsen and Chuang [8]. For completeness, we provide a self-contained proof.

Proof. We proceed via a probabilistic method. That is, we compute the probability that a random code has parameters $[[n, k, d]]$ with n large. To construct a random stabilizer code, we begin with $Z_1, \ldots, Z_{n-k}$ as stabilizers, and then choose a random Clifford operator U on n qubits. The random stabilizer code is given by $S_1 := U Z_1 U^\dagger, \ldots S_{n-l} := U Z_{n-k} U^\dagger$. Such a code is a uniformly random stabilizer code because (a) all generators commute and (b) a random Clifford takes distinct non-Identity Paulis to uniformly random non-Identity Paulis.

Fix a n-qubit non-Identity Pauli P and note that $P' := U P U^\dagger$ is a fixed uniformly random non-Identity Pauli. Let $p = \Pr[[P, S_1] = 0, \ldots, [P, S_{n-k}] = 0] = \Pr[[P', Z_1] = 0, \ldots, [P', Z_{n-k}] = 0]$ be the probability that P commutes with the stabilizer tableau. If P' commutes with Z_i, then the Pauli on the ith qubit must be either I or Z. There are $2^{n-k} 4^k - 1$ non-identity Paulis which have I or Z on the first $n - k$ qubits, and $4^n - 1$ total non-identity Paulis. For large n then,

$$p = \frac{2^{n-k} 4^k - 1}{4^n - 1} \approx \frac{2^{n+k}}{4^n} = \frac{1}{2^{n-k}}. \tag{C1}$$

On the other hand, the total number of non-identity Paulis with weight at most d is

$$N = \sum_{j=1}^{d} 3^j \binom{n}{j} \leq d 3^d \binom{n}{d}, \tag{C2}$$

using the assumption that $d \leq \frac{n}{2}$ so that the last term is the greatest. By Stirling's approximation,

$$N \longrightarrow 2^{nH(d/n) + d \log 3 + O(\log n)}. \tag{C3}$$

To complete the proof, we apply the union bound. Let $A(S, P)$ be the event that P commutes with $S_1, \ldots, S_{n-k}$, and let $A(S) = \bigcup_{P \neq I} A(S, P)$. Then

$$\Pr[A(S)] \leq \sum_{P \neq I} \Pr[A(S, P)]$$
$$\leq 2^{nH(d/n) + d \log 3 + O(\log n)} 2^{k-n}. \tag{C4}$$

A $[[n, k, d]]$ code exists if and only if $\Pr[A(S)] < 1$. By setting the right-hand side of Eqn. (C4) to < 1 and solving, we obtain the quantum Gilbert-Varshamov bound. $\qquad\square$